

Influence of Dissolved Organic Matter on the Photodegradation of Proteins

Assessing the Singlet Oxygen Reactivity of Histidine Residues in a Protein

Master Thesis

Author(s):

Schälchli, Jeremy

Publication date:

2013

Permanent link:

<https://doi.org/10.3929/ethz-a-010137093>

Rights / license:

[In Copyright - Non-Commercial Use Permitted](#)

ETH Zürich
Institute of Biogeochemistry
& Pollutant Dynamics

Master's Thesis

Influence of Dissolved Organic Matter on the Photodegradation of Proteins

Assessing the Singlet Oxygen Reactivity of Histidine Residues in a Protein

Jeremy Schälchli

May 2013

supervised by Prof. Kristopher McNeill
and Rachel Lundeen

Declaration of originality

I declare that this master's thesis *Influence of Dissolved Organic Matter on the Photodegradation of Proteins* is original work which I alone have authored and written in my own words, with the exclusion of proposed corrections, and that contributions from other sources are fully acknowledged.

Jeremy Schälchli

Abstract

The photo-oxidation of proteins in sunlit waters is complex. On the one hand, photo-oxidation kinetics of amino acid residues within proteins differ from freely dissolved amino acids, as for the former structural effects such as the accessibility of a photolabile residue to oxidants have to be taken into account. On the other hand, proteins in aquatic systems may undergo a variety of mechanisms that change their susceptibility to photo-oxidation, such as denaturation or encapsulation by dissolved organic matter (DOM).

To deal with this complexity, this work follows a reductionist approach. Using a well-defined experimental system and a well-characterized protein, glyceraldehyde-3-phosphate dehydrogenase (GAPDH), we found that the singlet oxygen reaction rate constant k_{rxn} of specific histidine (His) residues is governed by the accessibility of the residues to this oxidant. Moreover, proper k_{rxn} values for different His within GAPDH could be assessed.

Upon changing the experimental set-up to more natural conditions by using DOM as sensitizer for the production of singlet oxygen, we found that k_{rxn} values have changed, but were still in the same order of magnitude. We conclude from this finding that our model protein changed its conformation during DOM-sensitized photolyses. Thereby, formerly buried photolabile residues got more accessible and consequently more prone to photo-oxidation.

Studies following the Stokes shift in the fluorescence emission spectra of GAPDH

confirmed such conformational changes. A structural modification of GAPDH by DOM was also observed in the dark, but the process proceeded more slowly and less complete. The results suggest that these conformational changes in GAPDH were caused by direct interactions between DOM and the protein, but were enhanced by reactive species formed upon irradiation of DOM.

This work illustrates the complexity found when it comes to modelling processes affecting the fate of proteins in aquatic systems. Although literature often suggests that protein-organic matter interactions increase protein preservation in the environment, we find that these interactions, when occurring in sunlit waters, may also lead to enhanced photodegradation of the biomolecules.

Contents

1	Introduction	1
1.1	Motivation	1
1.2	Background	1
1.3	Studying photo-oxidation of GAPDH in a well defined system	2
1.4	Studying photo-oxidation of GAPDH in natural waters	4
2	Materials & Methods	7
3	Results & Discussion	13
3.1	Methylene blue-sensitized photolysis	13
3.2	SRNOM-sensitized photolyses	16
3.3	Fluorescence studies	20
3.4	Kinetic model	26
4	Conclusion	29
	Acknowledgments	31
	References	34
	Appendix	35

List of Figures

1.1	GAPDH crystal structure	3
1.2	GAPDH sequence, expected tryptic peptide fragments and His accessibilities	4
1.3	Scenarios for k_{rxn} ratio and values in system 2	6
3.1	Kinetic traces of His peptides in the MB-sensitized photolysis	14
3.2	Degradation rates of mono-His containing peptides plotted vs. $^1\text{O}_2$ -ASA of the His residue	15
3.3	Ratio of His54 and His108 k_{rxn} in system 1	15
3.4	Kinetic traces of His peptides in SRNOM-sensitized photolyses	17
3.5	Average His54 and His108 k_{rxn} in system 1 and 2	18
3.6	Logarithmic ratio of the normalized peptide intensities vs. measured $^1\text{O}_2$ - dose	19
3.7	Fluorescence emission spectra of photolysed GAPDH and SRNOM	21
3.8	Fluorescence emission spectra of GAPDH and SRNOM stirred in the dark	23
3.9	Fluorescence emission spectra of GAPDH in AmBic buffer photolysed and stirred in the dark	24
3.10	Kinetic model scheme	26
3.11	Kinetic model fits	27

1 Introduction

1.1 Motivation

Proteins are widely present in the environment^{1,2,3} and play a key role in the biogeochemistry of natural systems.⁴ They enter these systems as release of cellular constituents from living organisms or following cell death. Although proteins were historically considered to be very labile and transient in the environment, growing evidence suggests that a fraction may be preserved up to several decades.^{5,6,7}

The environmental chemistry of proteins is diverse and may include a variety of processes such as adsorption to mineral surfaces, absorption to organic matter, uptake by (micro-)organisms, and chemical modification. Knowledge about these processes is crucial for modelling nitrogen cycling dynamics, assessing the fate of prions, viruses or amino acid-based toxins, and understanding microbial exoproteomics and peptide uptake^{3,8,9}. A profound comprehension of the mechanisms affecting the degradation or preservation of proteins in the environment is therefore desirable. Unfortunately, many of these processes are only in the beginning stages of understanding.

This work takes a closer look at the photochemical oxidation of proteins in sunlit waters. The process is difficult to model because of two main reasons. First, photo-oxidation kinetics of amino acid residues within proteins differ from freely dissolved amino acids, as for the former structural effects such as the accessibility of a photolabile residue to oxidants have to be taken into account. Second, proteins in aquatic

systems may undergo a variety of mechanisms that change their susceptibility to photo-oxidation.

To elucidate the photo-oxidation of proteins in aquatic systems, we follow a reductionist approach. We will first assess the reaction rate constants k_{rxn} of specific histidine (His) residues within a model protein in a well-defined system (system 1). By doing so, we try to determine parameters that govern the differential reactivity of His residues within this protein. Having found these parameters, we will move on to a more natural system (system 2) and assess the same k_{rxn} there. The hypothesis is that based on our knowledge about these parameters we can interpret differences between the k_{rxn} in both systems to infer about mechanisms that change the susceptibility of proteins for photo-oxidation. These mechanisms need to be taken into account when it comes to modelling photochemical oxidations of proteins in the environment.

1.2 Background

The photochemical oxidation of proteins has been extensively studied in the context of cellular photobiology (as reviewed in Davies (2005)¹⁰). In cells, proteins are the major targets of photo-oxidation due to their abundance and high rate constants of several amino acids for reactions with photochemically formed oxidants.¹⁰

In general, photo-oxidation can occur via two different pathways. The first pathway,

called direct photo-oxidation, starts with absorption of one or more photons by the protein itself. The absorbed energy shuttles electrons into excited states which can ultimately lead to reactions that damage the protein. In cells, direct photo-oxidation by UVB ($\lambda = 280\text{-}320\text{nm}$) and UVA light ($\lambda = 320\text{-}400\text{nm}$) is restricted to tryptophan (Trp), tyrosine (Tyr), phenylalanine (Phe), histidine (His), cysteine (Cys), and cystine residues.¹¹

The second pathway, indirect photo-oxidation, is initiated with the absorption of light by a sensitizing compound. This sensitizer is usually transformed to an excited singlet state that quickly undergoes intersystem crossing to yield a triplet state. The triplet state may then either decay to its ground state, directly react with the protein, or transfer its energy to other molecules and thereby produce reactive species. These reactive species can react with some amino acids. If the triplet state transfers energy to molecular oxygen, this can lead to the formation of singlet state oxygen ($^1\text{O}_2$, molecular oxygen in its first excited state: $^1\Delta_g$). It is known that $^1\text{O}_2$ is highly selective for five amino acids: Trp, Tyr, His, Cys, and methionine.¹¹

Reaction rate constants for the oxidation of dissolved free amino acids with many oxidants including $^1\text{O}_2$ are known.¹² However, numerous photobiological studies indicate that these rate constants are different when amino acids are incorporated into a protein. These differences may be caused by a lowered accessibility of the residues within a protein or changes in the residues' local environment. Earlier studies have shown that amino acids at the surface of a protein are more prone to oxidation with $^1\text{O}_2$ than those buried within the protein.^{13,14} In another study, it was found that the $^1\text{O}_2$

quenching rate constants of two proteins were three and seven times lower than in mixtures of their constituent amino acids, but increased when the proteins were unfolded and thereby more accessible to the solvent.¹⁵ A recent paper investigated the $^1\text{O}_2$ -mediated oxidation of Trp in five proteins and found variability in their reaction rates. This variability was explained by a combination of different accessibilities and differences in the charge density, polarity or viscosity of the local environment of the Trp residues.¹⁶ All these studies indicate that photo-oxidation rates of amino acids within proteins may not be predicted accurately from reaction rate constants of dissolved free amino acids alone.

1.3 Studying photo-oxidation of GAPDH in a well defined system

A recent study in our group developed a method to quantitatively determine the $^1\text{O}_2$ reaction rate constants k_{rxn} for individual His residues within a model protein. $^1\text{O}_2$ is highly selective with a k_{rxn} of $1 \times 10^8 \text{M}^{-1}\text{s}^{-1}$ for dissolved free His¹². However, this study illustrated a differential reactivity for His residues within the model protein with k_{rxn} ranging from $1.54 \times 10^7 \text{M}^{-1}\text{s}^{-1}$ to $6.4 \times 10^7 \text{M}^{-1}\text{s}^{-1}$. Moreover, these k_{rxn} showed strong correlation with the calculated accessibilities of the His residues to $^1\text{O}_2$.

The model protein used was rabbit-muscle glyceraldehyde-3-phosphate dehydrogenase (GAPDH) (Figure 1.1), a homotetrameric enzyme with 11 His residues per subunit. GAPDH has a highly resolved crystal structure¹⁸ (2.4 Å resolution, PDB file 1J0X) that was used to compute His ac-

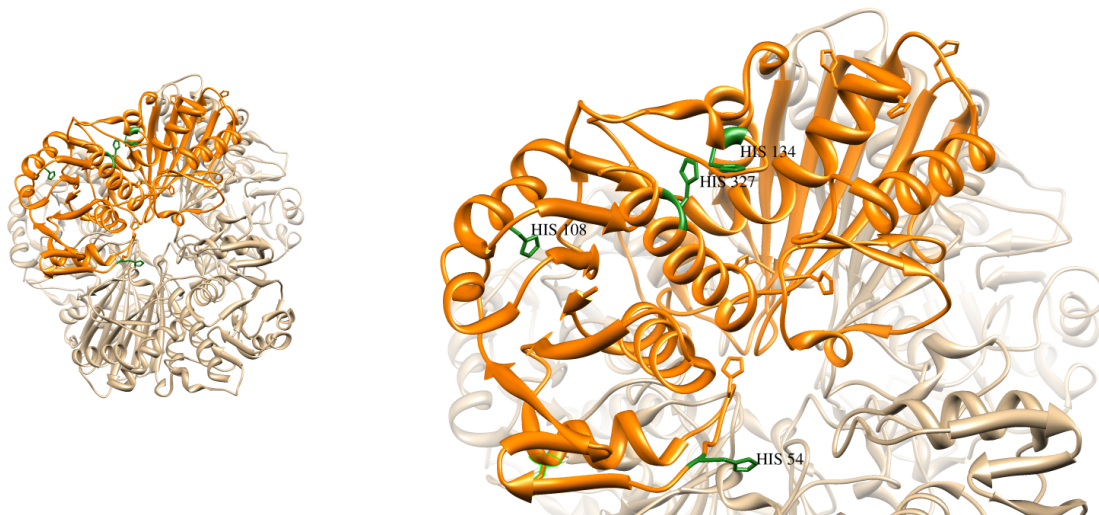


Figure 1.1: Structure of GAPDH, the model protein used in our studies. GAPDH is a homotetrameric enzyme with 11 His residues per subunit. One subunit is coloured and the four His residues of interest in this study are labelled. His54 is the most exposed, His108 the most buried residue. His134 and His327 are partially buried residues. The picture was generated with Chimera.¹⁷

cessibilities for $^1\text{O}_2$ with a designated software.¹⁹

Briefly, reaction rate constants k_{rxn} for His residues in GAPDH were determined by photolysing the protein in solution with methylene blue (MB), a synthetic sensitizer that has a high quantum yield for production of $^1\text{O}_2$ with visible light. Aliquots from the photolysis solution were taken at different time points and proteins within those aliquots were digested into shorter peptides using the proteases trypsin and chymotrypsin. Obtained peptides were quantitatively analysed on a liquid chromatography system coupled with a high resolution mass spectrometer (LC-HRMS). The degradation of peptides containing His residues were followed over the course of the photolysis and observed degradation rates were determined. In some cases, His was the only residue on those peptides that underwent significant oxidation with $^1\text{O}_2$

and thus peptide degradation rates could be equated with the $^1\text{O}_2$ -mediated oxidation rate of the contained His residue. This was also true for the peptides that contained the most exposed and most buried His residue after tryptic digestion (Figure 1.2a). Finally, k_{rxn} for specific His residues were obtained by dividing their oxidation rates by the measured steady state $^1\text{O}_2$ concentration ($[^1\text{O}_2]_{ss}$).

As the aim of this study was to determine k_{rxn} of residues with different, well known accessibilities, this set-up proved to be ideal. Firstly, the system was well-defined, as a well-characterized protein was used together with only MB as a sensitizer for $^1\text{O}_2$. MB does not sorb to GAPDH or disrupt its structural integrity (data not shown). Secondly, GAPDH provides the possibility to study 11 His residues within one protein. These residues span a wide range of accessibilities, from almost totally

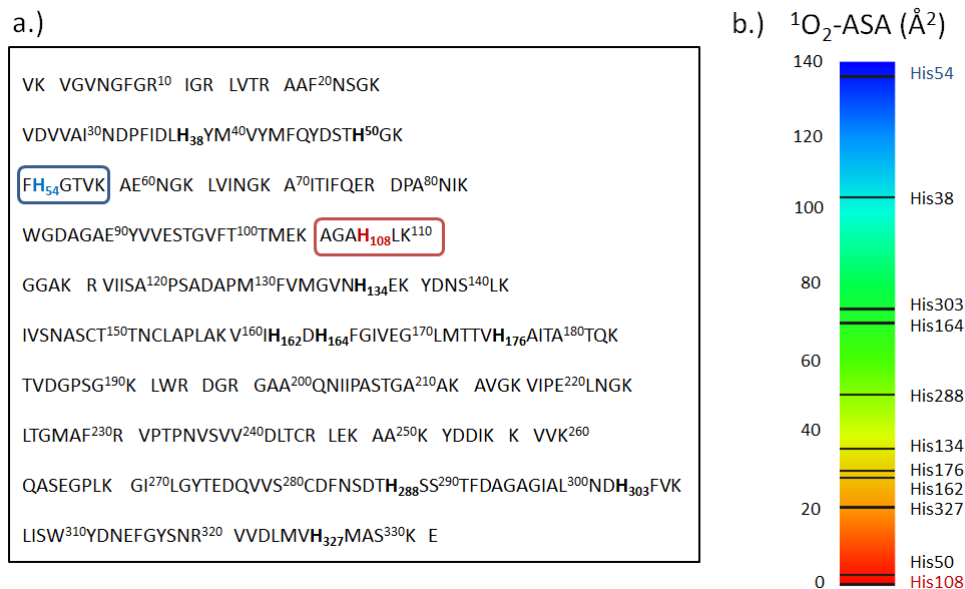


Figure 1.2: a.) Amino acid sequence of rabbit-muscle GAPDH. Predicted fragments from tryptic digestions are shown and the fragments with His54 (blue) and His108 (red) are highlighted. b.) $^1\text{O}_2$ accessible surface areas ($^1\text{O}_2$ -ASA) of His residues within GAPDH calculated using Getarea.¹⁹ $^1\text{O}_2$ -ASA of free His is 160\AA^2 .

exposed to completely buried ones (Figure 1.2b). Thirdly, the oxidation of dissolved free His with $^1\text{O}_2$ has a higher reaction rate constant than most other amino acids.¹² Finally, fluorescence studies indicate that GAPDH does not denature upon oxidation by $^1\text{O}_2$ in this system (Figure A.3).

Objective 1: Assessing $^1\text{O}_2$ reaction rate constants k_{rxn} of His residues in native GAPDH.

The first objective of this work is to reproduce k_{rxn} of four His residues in native GAPDH using this well defined system (system 1). The purpose is to further support the concept that within a protein accessibility to $^1\text{O}_2$ is the main parameter that determines k_{rxn} of His with this oxidant. Moreover, we want to assess the proper k_{rxn} values for the most exposed and most buried His residue (His54 and His 108,

respectively). This will lay the foundation on which we can draw conclusion from similar experiments in more natural systems.

1.4 Studying photo-oxidation of GAPDH in natural waters

Studying photo-oxidation of proteins in natural waters is more complex. As mentioned before, proteins in these systems are susceptible to various processes and influences from other constituents present in the environment.

One of the key players in aquatic systems is dissolved organic matter (DOM). DOM is a mixture of structurally not well defined macromolecules that stem from biological sources. These macromolecules tend to form colloids in aqueous solutions due

to hydrophobic interactions between their apolar moieties.²⁰ Consequently, the interior of these colloids is thought to be apolar, whereas the surface is often negatively charged at high and medium pH due to deprotonated carboxyl groups.

DOM is also the main sensitizer in aquatic systems. Irradiation of DOM leads to the formation of several reactive intermediates such as $^1\text{O}_2$, hydroxyl radicals ($\text{OH}\cdot$), hydrogen peroxides (H_2O_2), and triplet-excited states within the DOM (^3DOM).²¹ Due to their high reactivity and corresponding short half lives, concentrations of these compounds in natural waters are generally low. Singlet oxygen concentrations $[\text{}^1\text{O}_2]_{ss}$ between $(5 - 25) \times 10^{-14}\text{M}$ were measured, whereas $\text{OH}\cdot$ concentrations were calculated to be around $2 \times 10^{-16}\text{M}$ (data from Swiss lakes and rivers, 47.5°N , at noon time on a summer day).^{22,23} However, it was shown that $[\text{}^1\text{O}_2]$ are more than 100 times increased within DOM colloids and enhanced in a corona around them.²⁴ This implies that molecules which may sorb to DOM (such as apolar or positively charged compounds) may experience a much higher exposure to $^1\text{O}_2$.

Boreen et al. (2008)²⁵ examined the degradation of 18 dissolved free amino acids in natural water samples. Under environmental conditions, direct photo-oxidation of dissolved amino acids was observed for Trp and Tyr, whereas indirect photo-oxidation was found for Trp, Tyr, His, and Met. The indirect photochemical degradation of these four photolabile amino acids could be attributed to reactive species for various water samples and types of DOM. Oxidations of Trp, Tyr and Met were assigned to a combination of different oxidants, whereas His degradation occurred almost completely by oxidation with $^1\text{O}_2$.

This last finding with dissolved free amino acids opens the possibility to use the same system as before to test the differential reactivity of His residues within GAPDH when DOM is the sensitizer. In such a system (system 2), more reactive species will be involved. This makes it harder to attribute the degradation of peptides to the oxidation of a specific amino acid with a particular reactive species. However, it is possible to determine the reaction rate constants of the most exposed and most buried His residue, as they are the only photolabile amino acids on their containing peptides (Figure 1.2a) and His is expected to react with $^1\text{O}_2$ alone.

Objective 2: Assessing $^1\text{O}_2$ reaction rate constants k_{rxn} of the most exposed and most buried His residues in GAPDH using DOM as sensitizer.

The purpose of these studies is to help uncover mechanisms surrounding the influence that DOM has on the photo-oxidation of proteins. Comparisons between k_{rxn} for the most exposed (His54) and most buried (His108) His residues of GAPDH obtained in system 1 and 2 will allow to infer about interactions between GAPDH and DOM. We can differentiate between three cases (Figure 1.3):

1. Values and ratio of k_{rxn} stay the same. As it was found that the k_{rxn} of individual His residues are governed by their particular accessibility (objective 1), a constant ratio (and values) indicates that GAPDH in system 2 is still in the same conformation, its native state, and exposed to a $[\text{}^1\text{O}_2]$ as it is measured in the bulk aqueous phase.
2. The ratio of k_{rxn} has changed, but their absolute values are about the same. Following the above logic, a

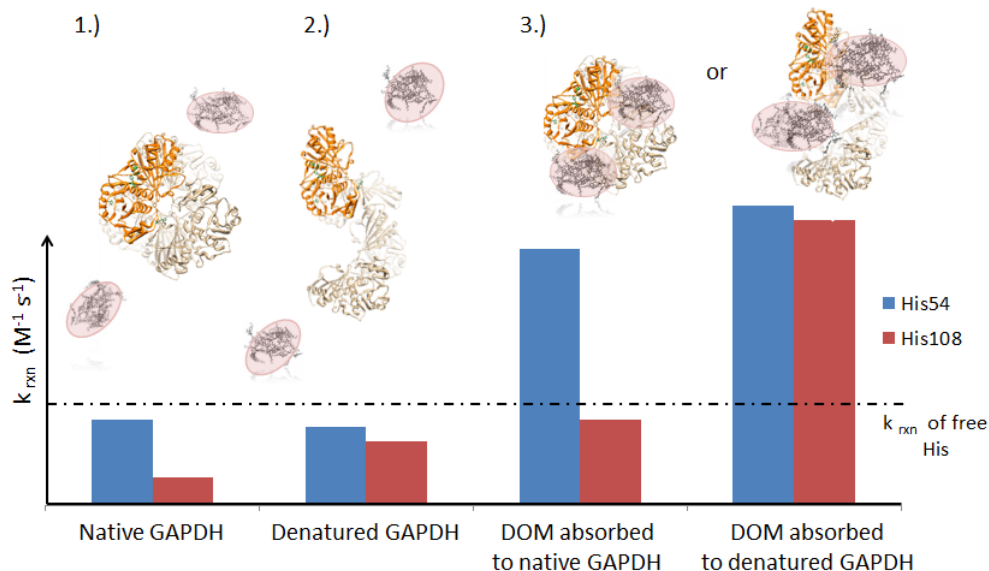


Figure 1.3: Different scenarios for k_{rxn} of His54 and His108 with DOM as sensitizer. The k_{rxn} under case 3.) might be more enhanced than displayed. The three scenarios are discussed in the text.

changed ratio denotes that accessibilities of His residues have changed, which is equivalent of saying that GAPDH has changed its conformation.

3. Absolute values are drastically increased compared to system 1 and higher than k_{rxn} of dissolved free His. Such enhanced k_{rxn} denote that His residues are exposed to a significantly higher $[^1O_2]$ than what we measure in the bulk aqueous phase and we therefore overestimate these k_{rxn} . As mentioned before, higher $[^1O_2]$ are found in and around DOM colloids. Thus increased k_{rxn} may indicate that DOM sorbs to GAPDH or even encapsulates the protein.

To test conclusions that we draw from this comparison, more experiments and a computational model will be set up.

2 Materials & Methods

Materials

Unless indicated otherwise, all chemicals were obtained from Sigma (Buchs, Switzerland) and used without further purification. Solutions were prepared using fresh 18M Ω water (MQ) from a Barnstead Nanopure Diamond Water Purification System.

We used Suwannee River Natural Organic Matter (SRNOM) as model DOM as it comprises a broad class of humic substances present in fresh water systems. SRNOM was obtained from the International Humic Substances Society (St. Paul, MN, USA). A 100mgC/l stock solution was prepared according to the following protocol: 9.98mg SRNOM was dissolved in 45ml MQ water and sonicated for 10 minutes. The pH was adjusted to 9.3 by adding 45 μ l 1M NaOH and the solution was sonicated again for 10 minutes before pH was adjusted to 7.35 by adding 12 μ l 1M HCl. The solution was stored over night at 4°C. On the next day, the solution volume was increased to 50ml by adding MQ and filtered through a sterile syringe filter (0.2 μ m cellulose filter, VWR International) using a dedicated pipette (50ml, Braun Omnifix). The solution was then transferred to LoBind Eppendorf tubes and stored at -21°C until 2 hours prior to use.

A methylene blue (MB) stock solution was prepared in MQ water at a concentration of 0.6mM and stored at 4°C. Furfuryl alcohol (FFA) was obtained from Merck (Germany), distilled and stored under argon. FFA stock solutions were pre-

pared fresh every week in MQ water to yield concentrations of 86.1mM and stored under Argon at 4°C. Ammonium bicarbonate (AmBic) was obtained from Fluka (Switzerland) and a new AmBic buffer solution (50mM, filtered with a 0.2 μ m cellulose filter) was prepared each day and adjusted to pH 7.8 using 37% concentrated HCl at room temperature.

Rabbit-muscle (*Oryctolagus cuniculus*) GAPDH was obtained as a lyophilized powder (Sigma, G2267-1KU) and stored at -21°C. GAPDH stock solutions were prepared fresh everyday in AmBic at concentrations of 1-2mg/ml. The solutions were prepared in LoBind Eppendorf tubes and kept on ice in the dark until use.

Sequencing grade modified trypsin (Madison, WI, USA) was prepared in LoBind Eppendorf tubes as recommended by Promega and stored at -21°C. Aliquots were thawed on ice in the dark 2 hours before use.

Mobile phases for liquid chromatography (UPLC) were prepared fresh every two weeks or on demand. Mobile phases for peptide separation were: A.) MQ water with 10% acetonitrile and 0.1% formic acid (98%, Fluka, Switzerland) (for photolyses with SRNOM: MQ water with 3% acetonitrile and 0.1% formic acid) and B.) acetonitrile with 0.1% formic acid. Mobile phases for FFA analysis were A.) MQ water buffered with sodium acetate (15mM, pH=5.9, 0.2 μ m filtered) and B.) acetonitrile.

Photolyses

The following photolyses are discussed in this thesis:

1. MB-sensitized photolysis (system 1)
2. SRNOM-sensitized photolyses (system 2): 3 experiments
3. SRNOM + GAPDH photolysis for fluorescence measurements and dark control
4. Only SRNOM photolysis for fluorescence measurements and corresponding dark control
5. Only GAPDH photolysis for fluorescence measurements and corresponding dark control
6. Only GAPDH photolysis for direct photolysis control

Preparation of photolysis solutions: All photolysis solutions were prepared in borosilicate glass test tubes (12 x 75 mm). Photolysis solutions had a volume of 3ml and concentrations were as follows: GAPDH: 1.5 μ M (0.216mg/ml), FFA: 116 μ M, sensitizer: 10 μ M MB and/or 50mgC/1 SRNOM. The appropriate amounts of stock solutions and AmBic were mixed together and the solutions were vortexed slightly. The solutions were let sit in the dark for 15min before photolysis.

Light source: The light source for all photolyses was a Xe lamp (Newport, USA, Model 66906) equipped with a cut off filter from Edmund Industrial Optics. A 455nm cut off filter was used for photolyses with MB as primary sensitizer (1), whereas a 400nm cut off filter was applied for photolyses with SRNOM as primary sensitizer (2-4) or no sensitizer (5,6). Xe lamp intensities were measured using an externally calibrated Ocean Optics Jaz fiber optics probe to ensure reproducible and stable irradiation

during and across photolyses. The focus of the lamp was held constant for photolyses with the same sensitizer. However, it was changed to a six times higher light intensity (measured by the Jaz fiber optic probe located in the middle of the focus) when SRNOM was used as primary sensitizer and for direct oxidation control. Cork stoppered borosilicate tubes were always placed in identical positions in front of the lamp. The photolysed solution was constantly stirred (400rpm).

1. MB-sensitized photolysis (system 1) was conducted for 35min. 150 μ l samples were taken at 0, 3, 5, 7, 10, 15, 25, and 35min, but the 0min measurement had to be dismissed because of wrong sampling. The samples were split immediately in two different 0.5ml LoBind Eppendorf tubes and stored in the dark on ice. One aliquot (23.2 μ l) was destined to undergo trypsin digestion and peptide analysis, whereas the other one was used for FFA degradation and [$^1\text{O}_2$] measurement. Microwave digestions were started between 7 and 10min and after 35min. pH of the photolysis solution was 8.0 \pm 0.1 at the start of the photolysis and increased to 8.3. The photolysis was conducted at 25 $^\circ$ C.

2. SRNOM-sensitized photolyses (system 2) were carried out for 7h 30min. Whereas in the first two executions 10 time points were sampled (150 μ l) (0, 30, 60, 120, 180, 240, 300, 360, 420, 450min), 13 time points were sampled in the third experiment (0, 20, 40, 60, 80, 100, 120 ... 450min). In the third experiment, FFA concentrations were not measured at all time points between 0-120min to decrease the amount of sample volume needed and guarantee comparable conditions with the other two experiments. Microwave digestions were started immediately after a time

point was sampled. pH of the photolysis solution were 8.0 ± 0.1 at the start of the photolysis and increased to 8.6 ± 0.1 . Photolyses were started at 25°C but temperature increased by about $5 \pm 1^\circ\text{C}$ during the experiment because of the higher light intensities.

3.-5. Photolyses for fluorescence measurements and corresponding dark controls: Three photolyses were conducted to trace shifts of fluorescence emission spectra. Additionally, corresponding dark controls were carried out. In the first round, GAPDH was mixed in SRNOM and irradiated for 2h (GAPDH+SRNOM). On the same day, SRNOM alone was photolysed for 2h (SRNOM only). Samples of $300\mu\text{l}$ were taken at 0, 5, 10, 15, 20, 40, 60, and 120min and transferred to a $0.5\mu\text{l}$ LoBind Eppendorf tube. Fluorescence emission spectra were measured immediately.

Additionally, four control experiments were conducted. These included the photolysis of a solution with no sensitizer (GAPDH only) and three dark controls (GAPDH+SRNOM, SNOM only, GAPDH only). All control experiments lasted 8h and were done on the same day, only few minutes time shifted. Samples were taken as described before and measured immediately. If this was not possible (concerns some dark control samples), they were stored in a dark ice box for some minutes.

6. Direct photolysis control: GAPDH dissolved in AmBic was irradiated for 450min with no externally added sensitizer. Results are given and discussed in the Appendix.

Microwave-assisted GAPDH digestion and peptide analysis

GAPDH digestions were initiated by spiking $2\mu\text{l}$ of $0.1\mu\text{g}/\mu\text{l}$ trypsin stock solution to the $23.2\mu\text{l}$ aliquots. This yielded a protein-to-protease (S/E) ratio (w/w) of 25:1. The aliquots were immediately vortexed and centrifuged (10s, $3'000\text{rpm}$). Digestions were conducted in a CEM Discovery system (CEM GmbH, Germany) for 10min at 50°C and 100W. Temperature was controlled with a fiber optics probe. Sample tubes were then stored in the dark for 15min to cool down to room temperature before digestion was stopped by lowering the pH below 3 with the addition of $0.5\mu\text{l}$ glacial acetic acid. Upon addition of the acid, samples were twice vortexed and centrifuged (10s, $3'000\text{rpm}$). $12\mu\text{l}$ were transferred into Waters Total Recovery LC vials. Analysis of digested samples was always carried out on the same day.

For peptide separation, $3\mu\text{l}$ of sample was injected to a LC system (Waters nanoAcquity UPLC) with a NanoEase Acquity BEH130 C_{18} column ($1.7\mu\text{m}$, $300\mu\text{m}$ x 150mm , 35°C) and a NanoAcquity UPLC C_{18} trapping column ($180\mu\text{m}$ x 20mm), but trapping was never applied in these experiments. The flow rate was $5\mu\text{l}/\text{min}$. Details about applied gradients can be found in the Appendix.

Peptide fragments were measured in a high resolution Orbitrap mass spectrometer with an Electrospray Ionization interface (ESI). All analyses were carried out in positive ionization mode. The instrument was calibrated every day. The ESI operated with a spray voltage of 4.4kV and at a capillary temperature of 27°C . High resolving power was applied within a scan range of $180\text{-}2500\text{m/z}$. Data was acquired by analysing the obtained mass spectra

with Thermo Xcalibur software.

The online tool PeptideMap (PROWL, Rockefeller University) was used to obtain predicted tryptic digestion fragments and their corresponding monoisotopic masses. Peptides with 0 - 2 missed cleavage sites were considered. M/z values for charges from 1+ to 5+ were calculated from the monoisotopic masses (Table A.3). An Excel file was set-up that contained all peptide fragments at different charge states and the corresponding m/z values. ToxID software (Thermo) searched for those values in the mass spectra and showed their peaks and retention times (RT). The peaks were validated by checking their high resolution m/z value and isotopic pattern in Xcalibur. Subsequently, the Excel file was refined by adding RT as criteria for semi-quantitative analysis by ToxID. This procedure was repeated the mobile phase gradient was changed to analyse SRNOM-sensitized photolyses.

Peak areas were used for quantification under application of an exact mass window of 5ppm and a RT window of 5min. Blank samples were always run. Digestion of only SRNOM in AmBic did not yield signals that interfere with peptides of interest.

Peptide degradation measurement, standardization and reaction rate constants

Although HRMS spectra were searched for m/z values of all predicted peptides, we only followed the degradation of peptides that contained the His residues located in the primary sequence at position 54 (His54, most exposed His residue), 108 (His108, most buried His residue) 134 (His134), and 327 (His327)(His peptides).

Two unreactive peptides were used as internal standards. In the MB-sensitized

photolysis, these standard peptides were 18-24 (charge states +1, +2) and 198-212 (+1,+2,+3) whereas in all photolyses that contained SRNOM the peptides 18-24 (+1,+2) and 184-191 (+1,+2) were used as internal standards as they were eluting at similar times as the His peptides. The MS intensities of His peptides at a specific time point were divided by a normalization factor (NF), which was calculated as the average recovery of the standard peptides at this time point compared to the maximum intensity of the respective standard peptide over the course of the experiment:

$$NF_t = \frac{\sum_{i=0}^n (Intensity_{i,t} / \max_{t=0}^T (Intensity_{i,t}))}{n}$$

where i is the index for a standard peptide m/z value, n is the number of standard peptide m/z values (5 and 4, respectively), t is a specific time point, and T the total amount of time points sampled.

The intensities of His peptides were normalized by their intensity at the start of the experiment (t_0 measurement). An exception to this is the MB-sensitized photolysis, where time point 1 (3min) was used for normalization because the t_0 measurement had to be dismissed due to wrong sampling.

Slopes of the linearized peptide degradations were calculated. A weighted average slope of all m/z values (multiple charge states) belonging to peptides containing a specific His residue was computed and used as average degradation rate for peptides containing this His residue. The weights were based on the overall intensity of a m/z value over the course of the experiment. His peptide m/z values that had very low intensities were not included in the calculation.

As mentioned in the introduction, we assumed that degradation of His peptides

was only due to the oxidation of the His residues with $^1\text{O}_2$. In the case of the His54 (peptide 53-58) and His 108 (peptide 105-110), this is justified as the His residue is the only amino acid on those peptides that undergoes significant reaction with $^1\text{O}_2$.¹² The other peptides that were followed (115-136 and 116-136, both His134; 321-331, and 321-332 both His327) contained additionally two Met residues, that might contribute to their degradation.¹² However, we expect the contribution of these Met to be small (see Section 3.1).

The oxidation of the His residues by $^1\text{O}_2$ is assumed to follow pseudo-first order kinetics as $[^1\text{O}_2]$ was kept constant:

$$\frac{d[\text{His}_{XY}]}{dt} = -k_{rxn, \text{His}_{XY}} * [^1\text{O}_2] * [\text{His}_{XY}]$$

where His_{XY} is a specific His residue and $k_{rxn, \text{His}_{XY}}$ the $^1\text{O}_2$ reaction rate constant of this residue.

The k_{rxn} of His54 and His108 were calculated by equating the averaged degradation rates of their containing peptides with $k_{rxn, \text{His}_{XY}} * [^1\text{O}_2]$ and dividing these degradation rates by the measured $[^1\text{O}_2]_{ss}$.

FFA degradation measurement and singlet oxygen concentration in the bulk aqueous phase

Aliquots designated for FFA analysis were centrifuged for 10min (10'000rpm) to (possibly) sediment GAPDH and SRNOM. 75 μl from the supernatant were transferred to vials. FFA degradation was measured on a Waters Acquity UPLC equipped with a photodiode array (PDA) detector, and these measurements were usually conducted on the same day as the experiment. 5 μl were injected on a Waters Acquity

UPLC HSS T3 (2.1mm x 150m; 35 °C) column for separation. The flow rate was 0.150ml/l and the gradient used for separation was isocratic with 35% sodium acetate and 65% acetonitrile. FFA signal was measured at a wavelength of 219nm. Every sample was injected twice. Interferences with residual SRNOM or GAPDH contained in the samples were ruled out with calibration experiments.

FFA degradation with $^1\text{O}_2$ follows pseudo-first order kinetics in the concentration range applied. The reaction rate constant used here was $8.3 \times 10^7 \text{M}^{-1} \text{s}^{-1}$.²⁶ Steady state singlet oxygen concentrations in the bulk aqueous solution were measured by dividing the slope of the linearized observed FFA degradation rate with this reaction rate constant.

Calculation of singlet oxygen accessible surface areas

Singlet oxygen accessible surface areas ($^1\text{O}_2$ -ASA) of His residues in our model protein GAPDH were calculated using the crystal structure of rabbit-muscle GAPDH¹⁸ (PDB file 1j0x, resolution 2.4Å). The crystal structure was submitted to GETAREA 1.1¹⁹ and $^1\text{O}_2$ -ASA of all His residues in all subunits were calculated using a 1.22Å probe radius (Table A.2). This probe radius was chosen based on the oxygen-oxygen bond length of 121.6pm of $^1\text{O}_2$.²⁷ Although they have the same amino acid sequence, the four subunits of GAPDH have been shown to have not an exactly identical structure.¹⁸ Therefore, we averaged $^1\text{O}_2$ -ASA values for a specific His residues over all four subunits.

Fluorescence measurements

Fluorescence measurements were conducted using a Fluorescence-3 fluorometer (Horiba, Jobin Yvon). Excitation and emission slit widths were 2.5nm and the measurements were conducted at room temperature. Samples were placed in a 300 μ l quartz microcuvette (Starna, Germany), not stirred, and excited first with a wavelength of 280nm while the emission spectra were recorded from 295 - 550nm. One minute later, a second measurement was conducted where samples were excited with 295nm and emission spectra were scanned from 305 - 550nm. At 280nm, Trp has its maximum absorbance and there is an onset of absorbance into Tyr.²⁸ Excitation at 295nm served to minimize this Tyr interference. In this study, we will mainly discuss the spectra acquired with excitation at 280nm because of the higher Trp fluorescence intensity which makes it easier to distinguish between protein and SRNOM fluorescence. Nevertheless, most spectral shifts could be reproduced with 295nm excitation. AmBic and MQ blanks were always measured before and after an experiment to check for drifting lamp intensities.

3 Results & Discussion

3.1 Methylene blue-sensitized photolysis

As mentioned under objective 1, the aim of this experiment is to reproduce data from an earlier study²⁹ (conducted by Rachel A. Lundeen, RAL). We use this well-defined system (system 1) to further strengthen the concept that the accessibility of a His residue is a main parameter in modulating its reaction rate constant k_{rxn} for the oxidation with $^1\text{O}_2$. Additionally, we want to assess the proper k_{rxn} values for the most exposed and most buried His residues in native GAPDH (His54 and His108, respectively).

Figure 3.1 shows the linearized degradation of six peptides over the course of the experiment. All six peptides contain one of four His residues. Correlation coefficients are generally high, indicating that the assumption of an exponential depletion due to a (pseudo-)first order kinetic following oxidation is reasonable. Furthermore, the degradation rates (the slopes) are different from each other but similar for peptides that contain the same His residue (Figure 3.1c & d, Table A.1 in the Appendix). For further discussion, peptides containing His134 or His327 are grouped together.

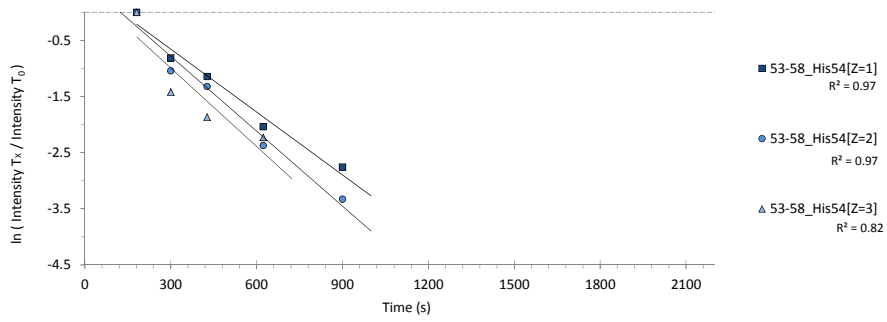
The observed $^1\text{O}_2$ reaction rate constants of these peptides determined from the averaged slopes and the measured $[^1\text{O}_2]_{SS}$ are shown in Figure 3.2 (red squares) together with data from RAL. In total, observed reaction rate constants of 14 different mono-His containing peptides from GAPDH and

free dissolved His are plotted against the $^1\text{O}_2$ accessible surface areas ($^1\text{O}_2$ -ASA) of the contained His residue. Generally, a strong correlation is found ($R^2=0.93$). An exception is the peptide containing His176, which shows a too high degradation rate constant and was not included in the calculation of the correlation coefficient. Possible explanations for this unusual high degradation rate are discussed elsewhere.²⁹

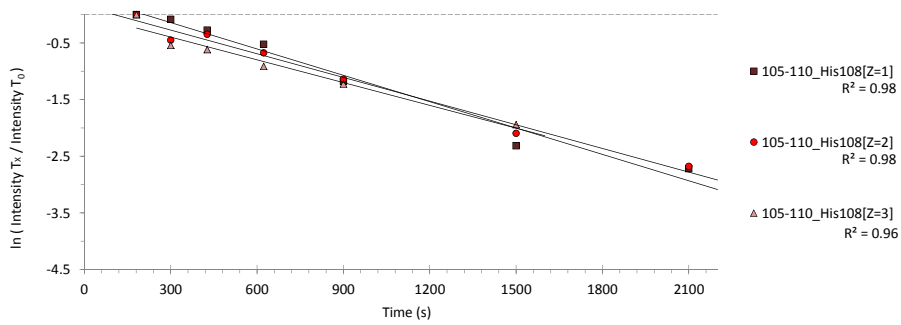
The strong correlation has a twofold meaning. First, it indicates that the His residues are the most important in terms of the $^1\text{O}_2$ reaction kinetics of these peptides.²⁹ This is consistent with the fact that free His has a much higher $^1\text{O}_2$ reaction rate constant than most other amino acids.¹² It seems therefore justified for our purpose to treat the observed reaction rate constants of the mono-His containing peptides as k_{rxn} of the respective His residues. Second, the strong correlation supports the concept that the calculated $^1\text{O}_2$ -ASA values play a major role in modulating the k_{rxn} of each His residue.

The new data from this study reproduces both the regression slope and the actual k_{rxn} values of the RAL data. Overall, both studies show that accessibility is a key parameter in controlling the $^1\text{O}_2$ k_{rxn} of His in GAPDH. This is one of the major findings that will help to interpret data from more complex systems (system 2). The other important results are the actual values for k_{rxn} of the most exposed and most buried His residues in native GAPDH.

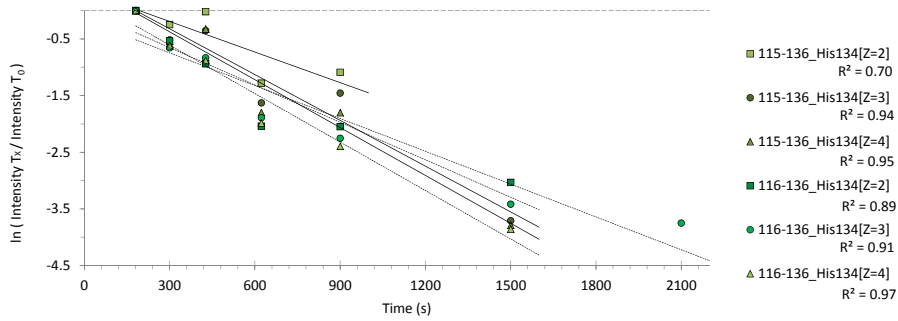
As discussed before, the tryptic peptides



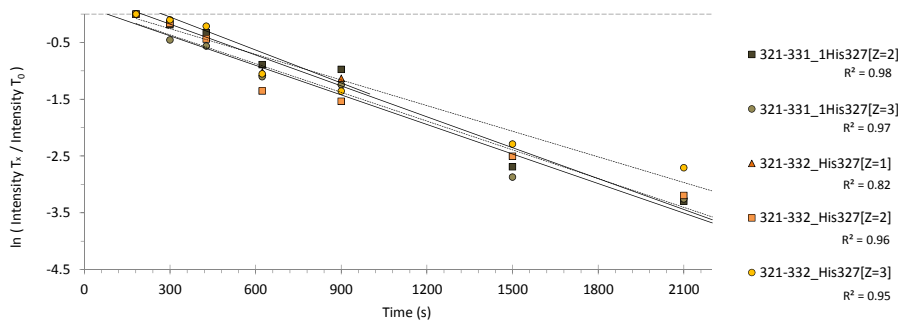
(a) Linearized degradation of peptides containing His54.



(b) Linearized degradation of peptides containing His108.



(c) Linearized degradation of peptides containing His134.



(d) Linearized degradation of peptides containing His327.

Figure 3.1: Linearized degradations of mono-His containing peptides from tryptic digestion of GAPDH during the MB-sensitized photolysis.

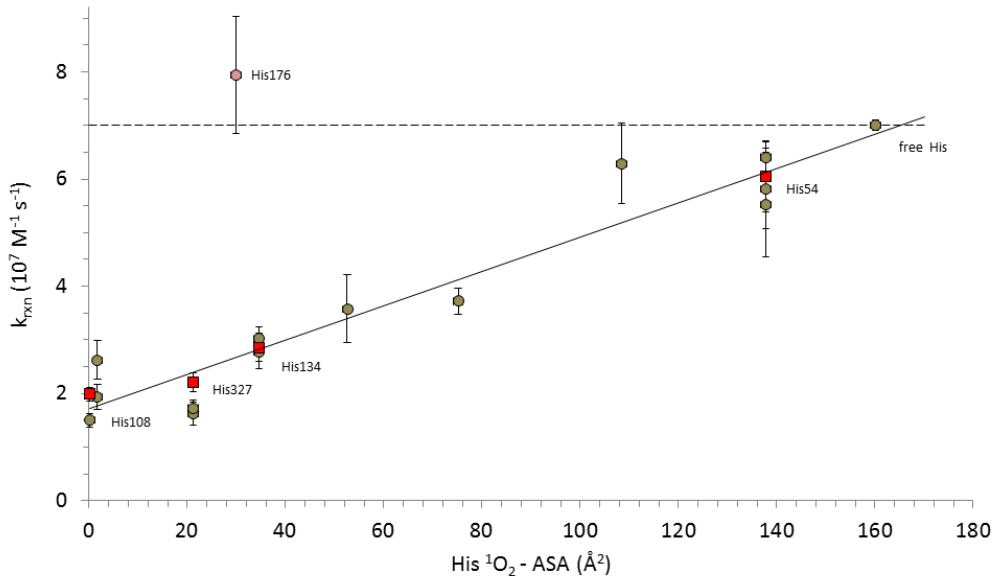


Figure 3.2: Observed $^1\text{O}_2$ reaction rate constants of 14 different mono-His containing peptides from GAPDH plotted versus the $^1\text{O}_2$ -ASA of the respective His residue. Data stem from RAL²⁹ (brown circles) and this study (red squares, peptides containing His134 and His327 are grouped together). The strong correlation ($R^2 = 0.93$, His176 containing peptide excluded) supports the assumption that His residues are the most important in terms of $^1\text{O}_2$ degradation of these peptides and that it is justified to treat the observed reaction rate constant of a certain peptide in many cases as the k_{rxn} of the contained His residue. Moreover, it indicates that $^1\text{O}_2$ -ASA is the parameter that governs the k_{rxn} of individual His residues in GAPDH.

containing His54 and His108 have no other amino acids on them that react significantly with $^1\text{O}_2$ (Figure 1.2); another justification to equate the observed $^1\text{O}_2$ reaction rate constant of these peptides with the k_{rxn} of the respective His residue. This yields a k_{rxn} of $6.05(+/-0.66) * 10^7 \text{M}^{-1} \text{s}^{-1}$ for His54 and $1.99(+/-0.13) * 10^7 \text{M}^{-1} \text{s}^{-1}$ for His108. Whereas the exposed His54 has a k_{rxn} which is almost as high as the one of free His ($7.00(+/-0.10) * 10^7 \text{M}^{-1} \text{s}^{-1}$)²⁹, buried His108 has a 3.5 times lower reactivity. The ratio between both k_{rxn} His54 and k_{rxn} His108 is 3.0. This illustrates again the profound impact of accessibility on the k_{rxn} of His residues within GAPDH. Moreover, the k_{rxn} values are in agreement with the ones from RAL (Figure 3.3).

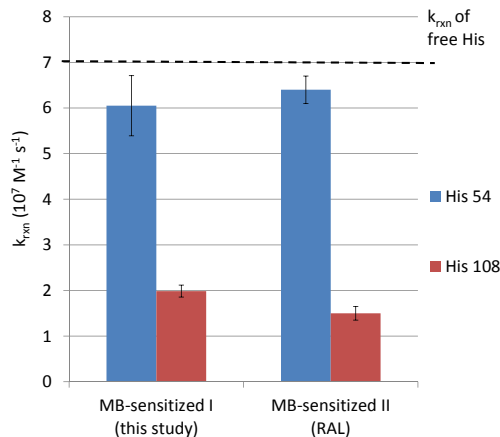


Figure 3.3: Ratio of His54 and His108 k_{rxn} in system 1 determined in this study and by RAL.

3.2 SRNOM-sensitized photolyses

Having confirmed that $^1\text{O}_2$ -ASA is a main parameter in modulating the differential reactivity of His residues to $^1\text{O}_2$ in GAPDH, we move on to a more natural system (system 2) by exchanging MB with SRNOM as sensitizer. As stated under objective 2, the goal is to assess the $^1\text{O}_2$ k_{rxn} of the most exposed and most buried His residues in GAPDH and compare these k_{rxn} with the ones obtained in system 1.

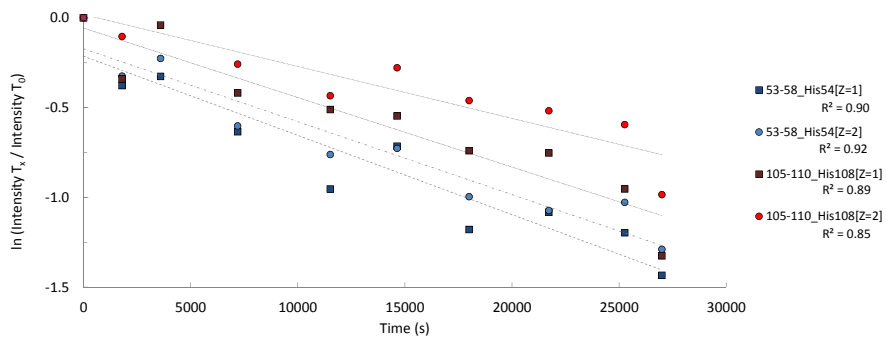
Figure 3.4 shows kinetic traces of the two most intense charge states of peptides containing His54 and His108 in all three conducted experiments. Degradation rates of these peptides are two orders of magnitude lower than in MB-sensitized photolysis due to a 100 times lower $[\text{}^1\text{O}_2]_{ss}$ (See Table A.1 in the Appendix for values). The linearized degradation shows some scattering that often affects all peptide intensities at one sampling time point similarly; an indication for the relatively big measurement uncertainty associated with our method compared to the degree of degradation. This measurement uncertainty made it necessary to conduct SRNOM-sensitized photolyses for 7.5 hours to get a quantifiable degradation.

As justified in the introduction, peptide degradation rates were equated with the $^1\text{O}_2$ oxidation rates of the contained His residues. Average k_{rxn} over the course of the photolysis were obtained by dividing the oxidation rates by the measured $[\text{}^1\text{O}_2]_{ss}$ (Table A.1). The k_{rxn} of His54 and His108 from all three experiments are shown in Figure 3.5. Overall, k_{rxn} of both His residues are enhanced. More remarkably, the ratio of the two k_{rxn} changed from 3:1 or 4.3:1 in system 1 to an average of

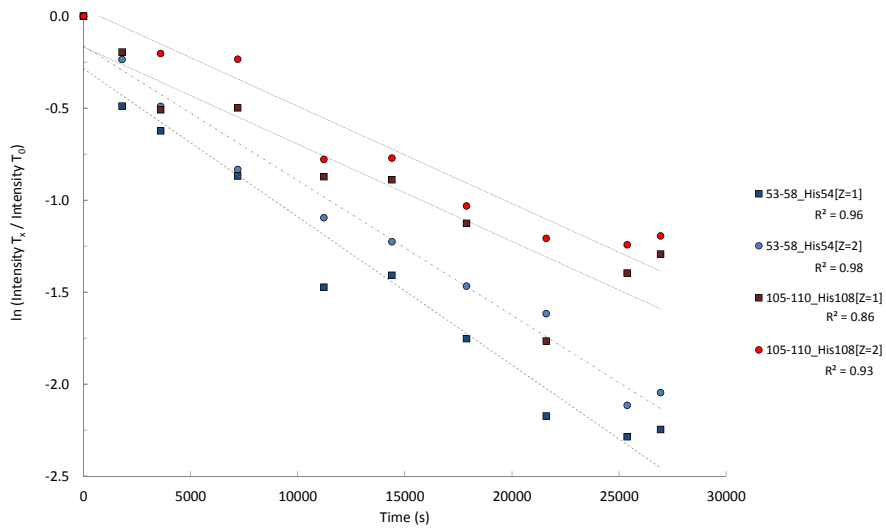
1.3:1 in system 2.

Based on our knowledge from system 1, we can interpret the altered ratios. Changes in the k_{rxn} ratio of the most exposed residue His54 and the most buried residue His108 indicate that their accessibilities have changed relatively to one another. In system 2, we find that the k_{rxn} ratio of His54 to His108 has decreased, which might be caused by a relatively decreased $^1\text{O}_2$ -ASA of His54 or a relatively increased $^1\text{O}_2$ -ASA of His108. As the k_{rxn} of both His residues (and especially His108) is enhanced, we assume that His108 has become more accessible. This increased accessibility of the formerly buried residue His108 indicates that GAPDH is no longer in its native state, but has changed its conformation or unfolded during photolyses with SRNOM.

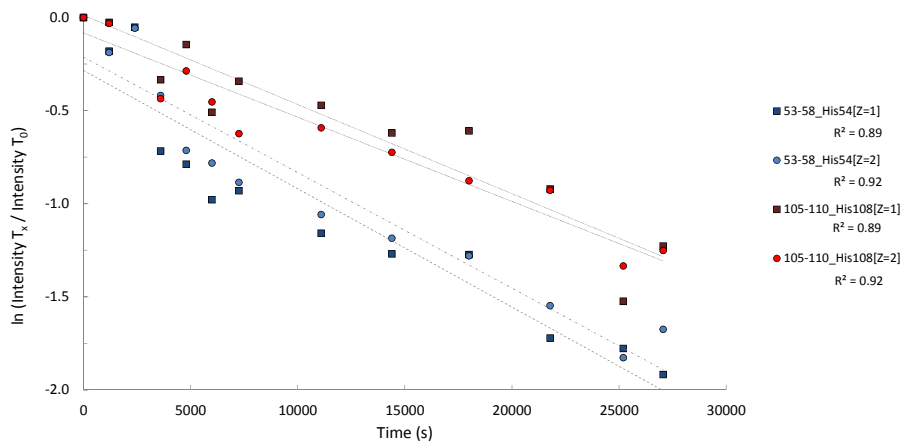
We also observe an increase in both k_{rxn} values. Notably, the k_{rxn} of His54 are higher than the $^1\text{O}_2$ reaction rate constant of free His. As discussed in the introduction, drastically enhanced reaction rate constant values may indicate that DOM is absorbed to the protein. This would lead to an underestimation of the $[\text{}^1\text{O}_2]$ in the residues microenvironment and thus to an overestimation of the k_{rxn} . However, $[\text{}^1\text{O}_2]$ in or around DOM are expected to be orders of magnitude higher than in the bulk aqueous phase²⁴ and consequently the effect on the k_{rxn} would have a similar scale. As there is only a slight enhancement and not an orders of magnitude difference between k_{rxn} of His54 in system 2 and free His, we cannot infer that SRNOM has substantially sorbed to GAPDH. The enhancement might more likely be caused by changes in the experimental conditions (temperature, pH) or by an only temporal or partial association of SRNOM with GAPDH.



(a) Linearized degradation of His54 and His108 containing peptides in experiment I.



(b) Linearized degradation of His54 and His108 containing peptides in experiment II.



(c) Linearized degradation of His54 and His108 containing peptides in experiment III.

Figure 3.4: Kinetic traces of tryptic peptides containing His54 and His108 in three SRNOM-sensitized photolyses.

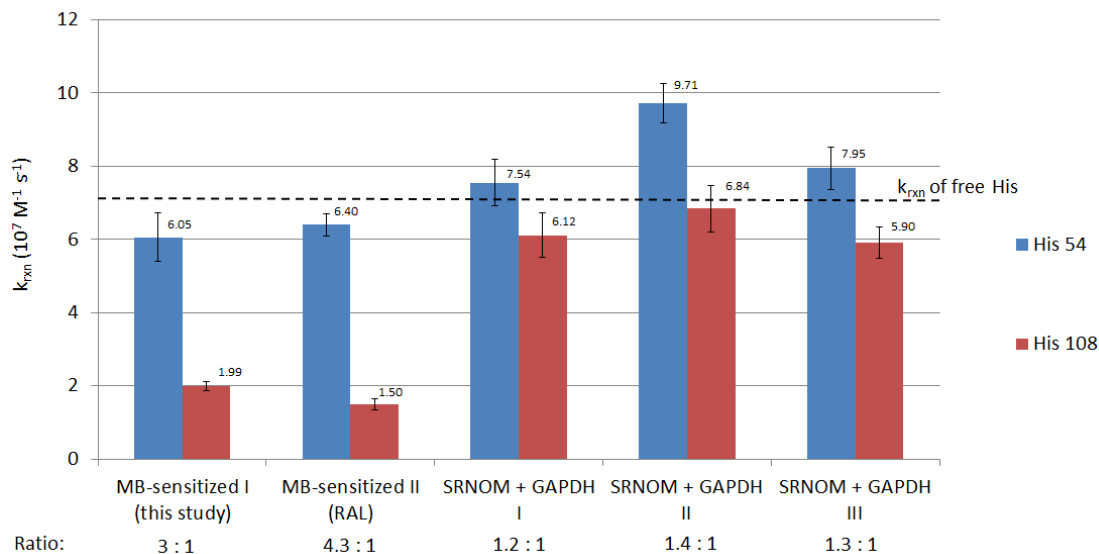


Figure 3.5: Average reaction rate constants k_{rxn} of His54 and His108 from MB-sensitized and SRNOM-sensitized photolyses.

It is important to note that the obtained k_{rxn} values depicted in Figure 3.5 are actually average or apparent reaction rate constants as they are calculated from the average degradation of His peptides over the full photolysis time. As we expect GAPDH to be in its native state at the beginning of each experiment, k_{rxn} at the start of a photolysis should be similar to those in system 1. However, these k_{rxn} in system 2 are not constant, but time dependent, $k_{rxn}(t)$, as they increase and their ratio alters when the conformation of GAPDH and the relative accessibilities of the His residues change.

Instead of looking at the averaged k_{rxn} and their ratio, we tried to observe changes in $k_{rxn}(t)$ over the course of a photolysis by sampling experiment III more frequently within the first two hours. The scattering makes it difficult to calculate appropriate degradation rates of single peptides for shorter time intervals than the full 7.5

hours (Figure 3.4c). However, the scattering seems to affect intensities of different peptides at one time point similarly. This allows it to still follow changes in the ratio of the two $k_{rxn}(t)$ over the course of the experiment. The logarithmic ratio of the normalized peptide intensities (LRNPI) should change in response to the 1O_2 -dose according to:

$$\frac{d(\ln(\frac{[His108]_t}{[His108]_0}) - \ln(\frac{[His54]_t}{[His54]_0}))}{d(t * [^1O_2])} =$$

$$k_{rxn,His54}(t) - k_{rxn,His108}(t)$$

(See Appendix for derivation of the formula.)

Data from experiment III and the MB-sensitized photolysis is shown in Figure 3.6. When plotted against the 1O_2 -dose, the LRNPI increases with the same slope in the starting phases of the two experiments. This is consistent with our assump-

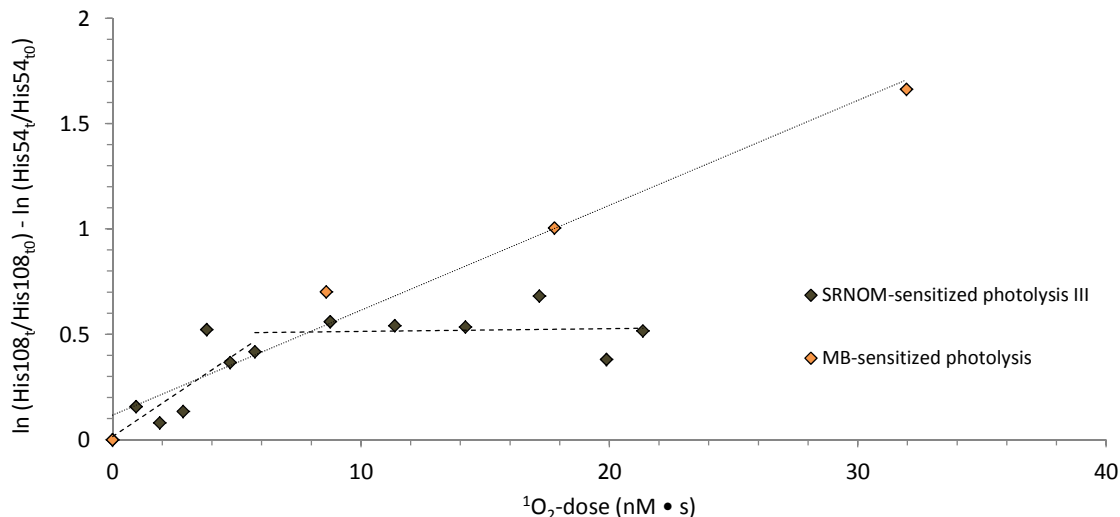


Figure 3.6: Logarithmic ratio of the normalized peptide intensities (LRNPI) versus $^1\text{O}_2$ -dose. The slope of the LRNPI is equal to the difference between $k_{rxn,His54}(t)$ and $k_{rxn,His108}(t)$. Whereas the LRNPI shows a constant increase in the MB-sensitized photolysis, it reaches a plateau in the SRNOM-sensitized photolysis III, indicating that $k_{rxn}(t)$ have changed over the course of this experiment and equalized after 2 hours.

tion that the $k_{rxn}(t)$ (and consequently their difference) in the beginning of the SRNOM-sensitized photolyses are equal to those in system 1 as GAPDH is still in its native state. In the MB-sensitized photolysis, the LRNPI continues to increase with a constant slope, indicating constant k_{rxn} over the whole experiment. However, in the SRNOM-sensitized photolysis, the LRNPI reaches a plateau after a $^1\text{O}_2$ -dose of 10^{-8}Ms (equals 2-3 hours in experiment III). The latter behaviour denotes clearly that the $k_{rxn}(t)$ of His54 and His108 change over time in system 2. Moreover, the observation that the LRNPI does not increase further might indicate that the two $k_{rxn}(t)$ have equalized after two hours

these $k_{rxn}(t)$ in system 2 are strong indications for a change in the conformation of GAPDH during SRNOM-sensitized photolyses. If the two k_{rxn} indeed have equalized after 2 hours, this would denote major structural changes of the protein. To further confirm the conformational change of GAPDH in SRNOM-sensitized photolyses and find its causes, fluorescence studies were conducted. Additionally, a computational model was set up to assess the $k_{rxn}(t)$ of His54 and His108 in structurally modified GAPDH.

Both the different ratios of average k_{rxn} of His54 and His108 between system 1 and 2 and the observed time dependency of

3.3 Fluorescence studies

Fluorescence spectroscopy is an established technique for studying the structure of proteins.²⁸ Changes in the conformation of proteins can be recognized by shifts in the Trp fluorescence emission maximum position (Stokes shift). This method has been applied to trace denaturation of GAPDH by Guanidine Hydrochloride before³⁰ and we could reproduce those results (shown in the Appendix). Whereas native GAPDH showed a maximum fluorescence emission at 337nm, the fully denatured protein had its emission peak at 354nm. We also used fluorescence emission to verify the structural integrity of GAPDH in system 1 (shown in the Appendix) and we will use it in system 2 to test the hypothesis that GAPDH is changing its conformation during SRNOM-sensitized photolyses.

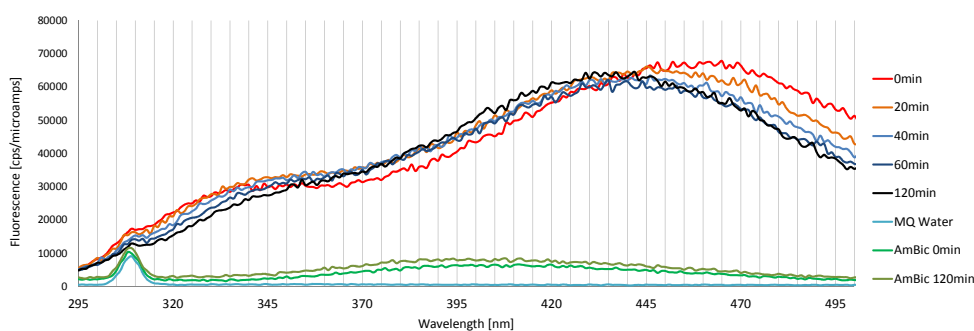
Figure 3.7a shows fluorescence emission spectra of GAPDH in SRNOM over the course of a two hour photolysis, whereas Figure 3.7b shows the spectra of SRNOM alone. It is apparent from a comparison between the two figures that the contribution of GAPDH to the total recorded fluorescence of system 2 is relatively small but recognizable in the range from 320nm to 370nm. The spectra in Figure 3.7b were subtracted from the corresponding spectra in Figure 3.7a to yield spectral contours of fluorescence attributed to GAPDH as shown in Figure 3.7c. This background subtraction was done at every time point separately to account for the spectral changes in the photolysed SRNOM solution, although major changes in SRNOM fluorescence during the photolysis are only observed in the range above 440nm. The resulting spectral contours of GAPDH fluorescence showed scatter (thin lines in Figure 3.7c), which

were smoothed by applying a Savitzky-Golay filter³¹ with a window size of 10 data points (bold lines in Figure 3.7c).

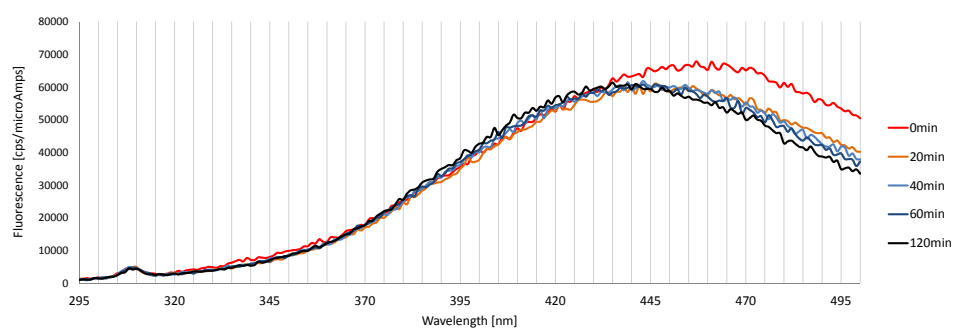
Therefore Figure 3.7c displays the change of GAPDH fluorescence emission over the course of a SRNOM-sensitized photolysis. The smoothed fluorescence emission spectrum of GAPDH at time point 0min has its maximum at 337nm. This is the same maximum emission wavelength as was found in system 1 and is in agreement with our previously confirmed assumption that GAPDH is in its native state at the beginning of the SRNOM-sensitized photolyses. Over the course of the experiment, the maximum shifts to 353nm, a peak position that is assigned to Trp residues fully exposed to water or free dissolved Trp and indicative of an unfolded GAPDH.

To our knowledge, this is the first time that fluorescence spectroscopy is used to trace denaturation or conformational changes of a protein in solution with DOM. The results seem promising, as a gradual shift in the emission maximum was observed over time. However, one of the problems associated with this method are inner filter effects. SRNOM absorbs both the exciting light (primary filter effect) as well as the fluorescence emitted by the protein (secondary filter effect). We tried to overcome these problems by 1.) exciting the solution at a wavelength where Trp has its absorbance maximum to increase GAPDH fluorescence and 2.) using a microcuvette with a short light path length to decrease filter effects (Figure A.5). Still, GAPDH fluorescence is considerably attenuated in comparison with the fluorescence of the protein in AmBic buffer (Figure 3.9).

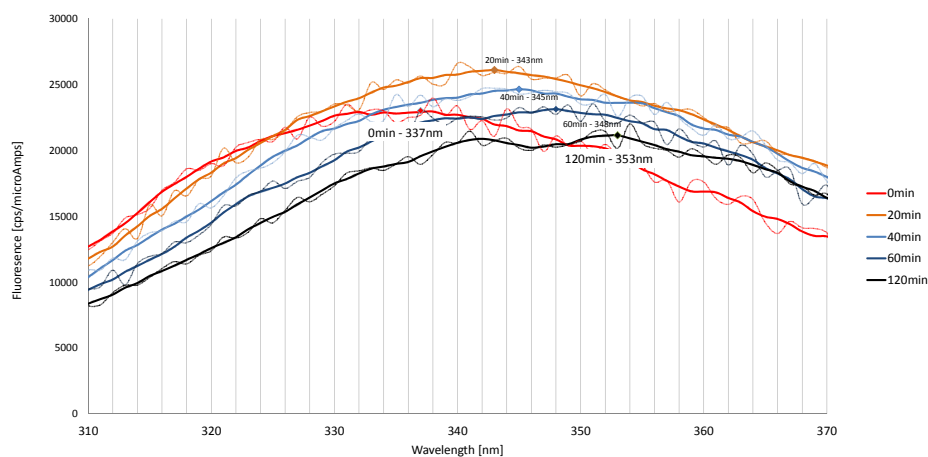
Although the inner filter effects affect the fluorescence intensity, we assume the wave-



(a) Fluorescence emission spectra of photolysed GAPDH in SRNOM.



(b) Fluorescence emission spectra of photolysed SRNOM.



(c) Fluorescence spectra attributed to GAPDH over the course of the photolysis.

Figure 3.7: Fluorescence emission spectra of (a) photolysed GAPDH ($1.5\mu\text{M}$) in solution with 50mgC/l SRNOM, (b) photolysed SRNOM (50mgC/l). The spectra in (c) were obtained by subtraction of corresponding SRNOM spectra from GAPDH in SRNOM spectra and display the fluorescence attributed to GAPDH. Thin lines represent the originally obtained curves; bold lines smoothed curves using a Savitzky-Golay filter (window size 10 data points). Excitation wavelength was 280nm . The solutions were irradiated under the conditions applied for SRNOM-sensitized photolyses and fluorescence spectra were recorded immediately after samples were taken.

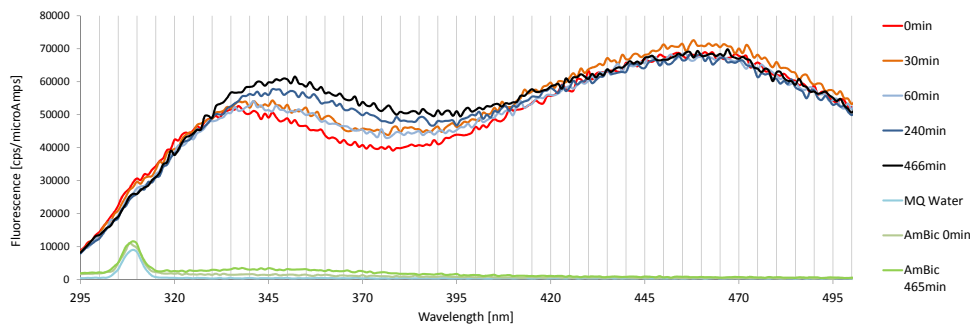
length of maximum emission to be reliable. First, in order to get misplaced emission peaks due to inner filter effects, a considerable gradient in the absorbance spectrum of SRNOM is required. This is not the case for our experimental set-up in the range of 320nm to 370nm (Figure A.5 in Appendix). Second, inner filter effects cannot explain the observed peak shift over time, unless the absorbance spectrum changes itself. We did not record absorbance spectra of SRNOM at different time points of the photolysis. However, changes in the absorbance spectrum, and thereby the inner filter effects, would become apparent as modifications in the fluorescence spectra of SRNOM. Yet, the SRNOM fluorescence spectra are unchanged over time in the range considered (Figure 3.7b). Third, the peak position obtained for time point 0min is the same as expected and known for native GAPDH, which shows that the method yields correct emission peak positions. We therefore conclude that the observed shift in fluorescence emission maxima are accurate.

The spectral shift is a strong indication that GAPDH changes its conformation or unfolds in SRNOM-sensitized photolyses. This is consistent with the results from section 3.2. However, such a conformational change may be caused by different factors. It is possible that interactions between SRNOM and the protein lead to modifications in the structure of GAPDH. Alternatively, reactive species other than $^1\text{O}_2$ produced by irradiation of SRNOM could have effects on the conformation of GAPDH.¹⁰ Besides, changes in the pH (8.0-8.6) and temperature (25-31 °C) over the course of the photolyses may disrupt the structural integrity of GAPDH.

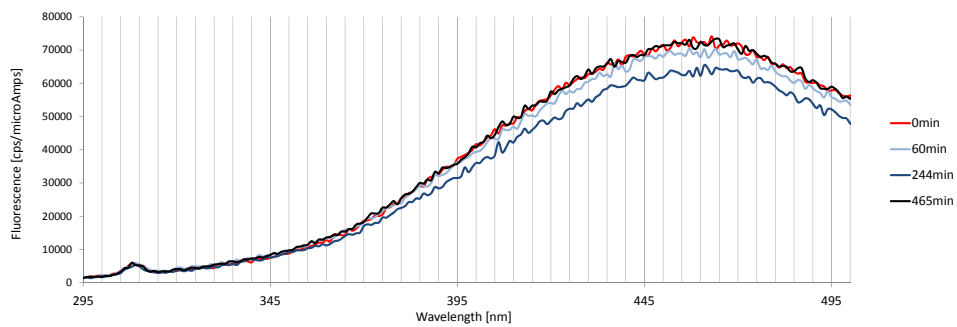
Control experiments

To elucidate the causes of the observed conformational changes, further fluorescence studies were conducted. An experiment was carried out where GAPDH in solution with SRNOM was stirred in the dark for 7hours 45min. Figure 3.8a shows fluorescence emission spectra of the solution recorded at different time points. In contrast to the photolysed solution (Figure 3.7a), changes in the emission spectra are mainly observed in the range of 330nm to 360nm. In a separate tube, SRNOM without GAPDH was stirred in the dark, aliquots were taken at the same time points and spectra were measured (Figure 3.8b.)). The emission spectrum at 240min shows lower intensities than all other time points, possibly as a result of missampling leading to a less concentrated sample. In general, no trend is observable and the spectra of dark SRNOM at 0min and 465min are overlapping. Having recorded fluorescence emission spectra of GAPDH in SRNOM and SRNOM alone, the same procedure as described before was applied to obtain spectral contours attributed to GAPDH fluorescence (Figure 3.8c). The emission peak of these spectra shifts from 336nm (0min) to 344nm within four hours, but not further for the rest of the experiment.

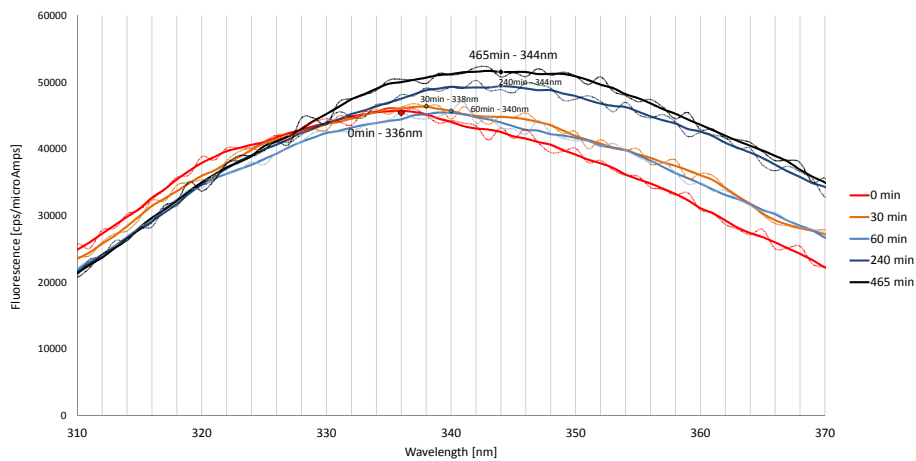
The second control experiment was conducted to test whether changes in pH and temperature can account for the observed conformational change of GAPDH. To this end, GAPDH was photolysed in AmBic buffer without added sensitizer. Additionally, a corresponding dark control experiment was carried out. The recorded spectra are shown in Figure 3.9. Emission peaks at the beginning of both photolysis and dark experiments showed emission maxima at 336nm. Throughout the GAPDH



(a) Fluorescence emission spectra of GAPDH in SRNOM stirred in the dark.

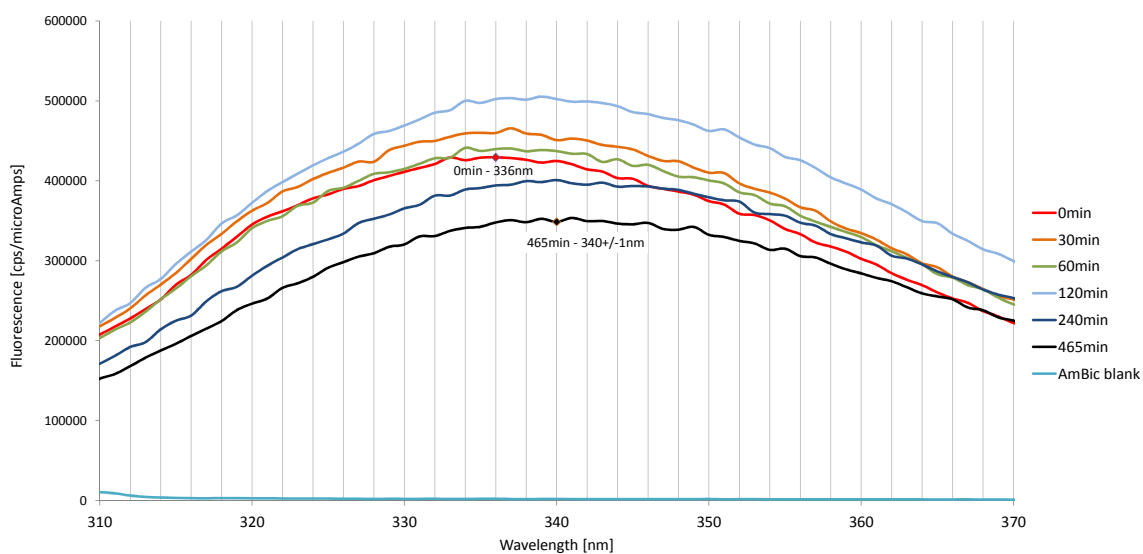


(b) Fluorescence emission spectra of SRNOM stirred in the dark for subtraction.

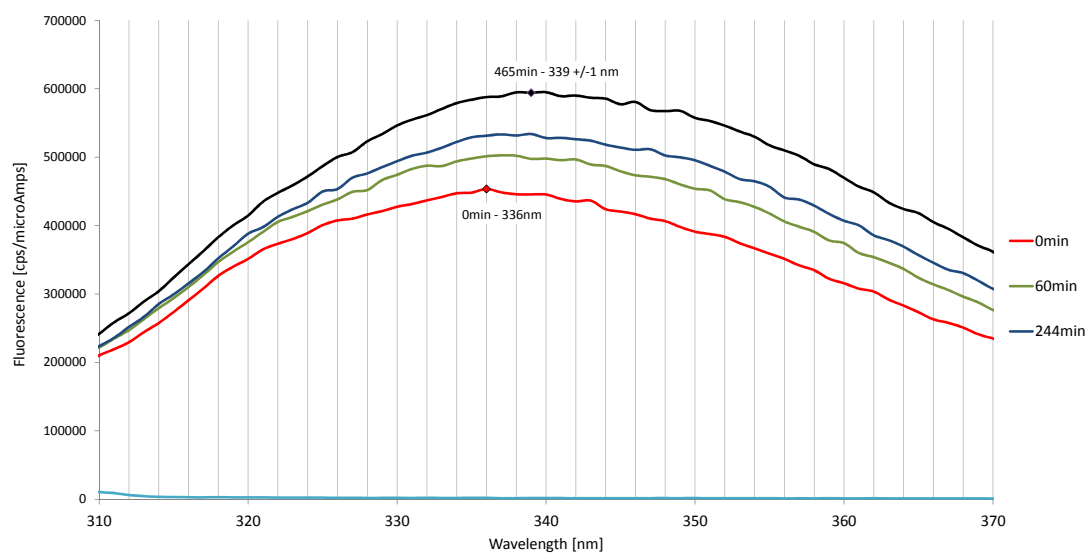


(c)

Figure 3.8: Fluorescence emission spectra of (a) GAPDH ($1.5\mu\text{M}$) stirred in the dark in solution with 50mgC/l SRNOM and (b) SRNOM (50mgC/l) stirred in the dark. The spectra in (c) were obtained by subtraction of corresponding SRNOM spectra (b) from GAPDH in SRNOM spectra (a) and display the fluorescence attributed to GAPDH. Thin lines represent the originally obtained curves; bold lines curves smoothed using a Savitzky-Golay filter (window size 10 data points). Excitation wavelength was 280nm . Fluorescence spectra were recorded immediately after samples were taken.



(a) Fluorescence emission spectra of photolysed GAPDH.



(b) Fluorescence emission spectra of GAPDH stirred in the dark.

Figure 3.9: Fluorescence emission spectra of (a) photolysed GAPDH ($1.5\mu\text{M}$) in AmBic buffer without added sensitizer, and (b) GAPDH ($1.5\mu\text{M}$) in AmBic buffer stirred in the dark. Excitation wavelength was 280nm. Fluorescence spectra were recorded immediately after samples were taken.

alone photolysis (Figure 3.9a), the fluorescence intensities fluctuated and resulted in a lower intensity at the end of the experiment with a slight shift in emission maximum to 340nm. In the dark, the fluorescence intensity gradually increased with a slight shift to 339nm within eight hours.

In all of these control experiments, small modifications in GAPDH conformation were expected due to experimental conditions. The temperature of the solutions changed from 4 – 10 °C, where GAPDH is most stable in solution, to room temperature or 30 °C. As well the pH increased from 8.1 to 8.6 nearing the isoelectric point of GAPDH.³² This small modifications are observable by slight fluorescence emission maximum shifts as in the GAPDH alone studies (Figure 3.9). However, in the dark experiment where GAPDH was in solution with SRNOM (Figure 3.8c) this shift is significantly enhanced, indicating a more pronounced conformational change of GAPDH.

Conclusions

Overall, fluorescence emission peaks of GAPDH shift significantly in experiments with SRNOM, both when irradiated and in the dark. This Stokes shift is only small when the protein is in solutions without SRNOM and under the same conditions. We conclude from these results that interactions of GAPDH with SRNOM are the main cause for changes in the conformation of the protein in system 2. These interactions may be either direct, via electrostatic and hydrophobic forces for example, or indirect, via reactive species produced upon irradiation of SRNOM. Our data suggests that both types play a role. On one side, a significant spectral shift is observed in the dark, where no reactive species are present,

indicating that the interaction or association of SRNOM with GAPDH contributes to the conformational change of the protein. On the other side, a more pronounced Stokes shift is observed in the SRNOM-sensitized photolysis than in the dark control experiment. This denotes that reactive species may further promote the conformational change, possibly leading to complete unfolding.

One thing to note here is that GAPDH has three different Trp residues and the obtained emission spectra are superpositions of the fluorescence spectra of all three residues. It is possible that the individual emission spectra of the Trp residues have different peak positions. Reactive species formed upon irradiation of SRNOM may lead to degradation of Trp residues in GAPDH. If such a degradation preferentially affects one specific Trp residue and thereby decreases its contribution to the whole fluorescence, this would complicate comparisons between the Stokes shifts of GAPDH in photolysed and dark SRNOM solutions over time. As we are not able to assess the degradation rates of all Trp residues, we cannot account for this effect. Nevertheless, as the fluorescence intensity does not substantially decrease over time in the photolysed solution, we do not expect this effect to play a major role.

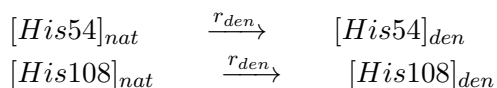
Overall, these fluorescence studies confirm our hypothesis that GAPDH changes its conformation during SRNOM-sensitized photolyses. We attribute these structural modifications mainly to interactions of the protein with SRNOM.

3.4 Kinetic model

In order to assess the oxidation kinetics of structurally modified GAPDH, a simple computational model was developed. The aim is to fit this model to data obtained from system 2 by means of a dedicated software, KinTek Explorer (KinTek Corporation, TX, USA).³³ Thereby we hope to find constrained, accurate values for the k_{rxn} in structurally modified GAPDH.

The model comprises two processes: the structural modification of GAPDH over time, here called "denaturation", and the oxidation of His54 and His108 residues both in native and structurally modified GAPDH. These two processes are broken up into six irreversible reactions as depicted in Figure 3.10.

The first two reactions represent the denaturation of GAPDH over time, separately affecting His54 and His108. Both reactions follow first order kinetics with the same rate constant r_{den} :



where $[His54]_{nat}$ and $[His108]_{nat}$ are the concentrations of unoxidized His54 and

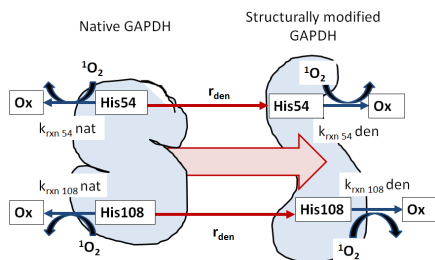
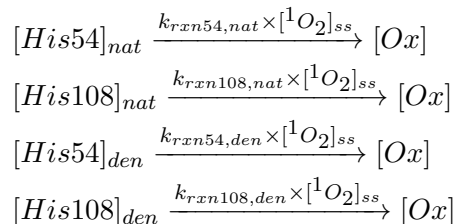


Figure 3.10: Scheme of the simple computational model used here.

His108 residues in native GAPDH, and $[His54]_{den}$, $[His108]_{den}$ concentrations of the respective unoxidized residues in structurally modified GAPDH.

The remaining four reactions are oxidations of His residues by 1O_2 . These reactions follow pseudo-first order kinetics:



where $[Ox]$ are not further defined oxidation products; $k_{rxn54,nat}$ and $k_{rxn108,nat}$ reaction rate constant of His54 and His108 in native GAPDH; and $k_{rxn54,den}$ and $k_{rxn108,den}$ the reaction rate constants of His54 and His108 in structurally modified GAPDH.

The data used for this fit stem from a SRNOM-sensitized photolysis (experiment III). As we cannot differentiate with our method between His residues in native or denatured proteins, the peptide intensities measured represent the sum of both. Therefore the observables are:

- Obs. 1: $[His54]_{nat} + [His54]_{den}$ and
- Obs. 2: $[His108]_{nat} + [His108]_{den}$

The intensities of the two most intensive charge states for both His containing peptides were summarized at every time point and these values were normalized to their intensity at time point t_0 . These normalized intensities of His54 and His108 containing peptides are shown as red (His54) and green (His108) points in Figure 3.11.

The initial estimates for all reaction rates are given in Table 3.1. The value for the

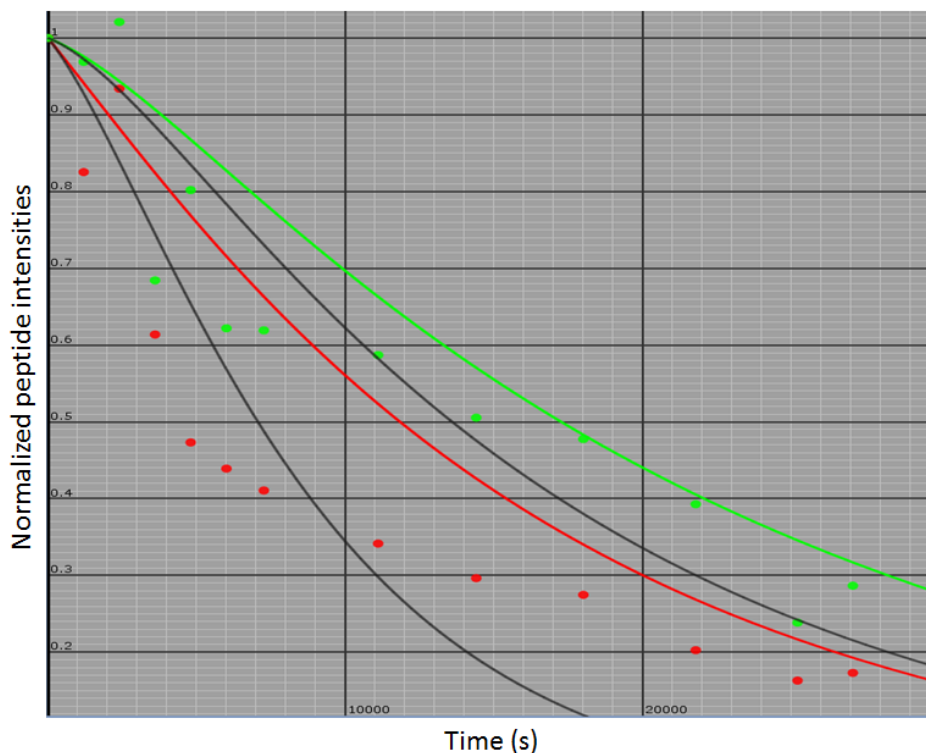


Figure 3.11: Fits of the described kinetic model to data from a SRNOM-sensitized photolysis. Red points: normalized intensities of His54 containing peptides. Green points: normalized intensities of His108 containing peptides. The grey lines display the best fits obtained with the initial values and restrictions described in the text. The red and green curves represent kinetic traces of the two observables based on the initial estimates.

denaturation rate r_{den} is based on the observation made in the fluorescence study, where the GAPDH fluorescence emission peak shifted to 353nm within 2 hours photolysis. Assuming that this position marks the completion of structural modification of GAPDH, we equated 120min with 3 half life times of the above process. The value is not fixed however, but allowed to adjust or "float".

The initial values for the k_{rxn} in native GAPDH were the ones obtained in this study and are fixed, as we assume them to be accurate. Although we do not know the k_{rxn} of His residues in structurally modi-

fied GAPDH and an assessment of these values is the actual aim of this fit, initial estimates for these have to be entered in order to conduct a nonlinear regression

Table 3.1: Initial estimates for rates and rate constants

rate	value	fixation
r_{den}	$2.9 \times 10^{-4} \text{s}^{-1}$	floating
$k_{rxn54,nat}$	$6.11 \times 10^7 \text{M}^{-1} \text{s}^{-1}$	fixed
$k_{rxn108,nat}$	$1.98 \times 10^7 \text{M}^{-1} \text{s}^{-1}$	fixed
$k_{rxn54,den}$	$7.95 \times 10^7 \text{M}^{-1} \text{s}^{-1}$	floating
$k_{rxn108,den}$	$5.90 \times 10^7 \text{M}^{-1} \text{s}^{-1}$	floating
$[^1O_2]_{ss}$	$7.89 \times 10^{-13} \text{M}$	

analysis. We therefore chose the average or apparent k_{rxn} from the third SRNOM-sensitized photolysis (Table A.1) as starting estimates.

Model, data and initial estimates or values of all parameters were entered to the software KinTek Explorer and a minimal χ^2 fit was conducted. The resulting best fitting curves for both observables are shown as grey curves in Figure 3.11, the underlying adjusted r_{den} and k_{rxn} values are given in Table 3.2.

As we did not assess the standard deviation of our data set, the obtained χ^2 value is only a relative indicator. The only criterion to assess the goodness of the fit is by eye.

It is clear that the fit does not follow the data well. Especially the His54 data is not well reproduced, as the fit fails to follow the "inverted-S" form of the intensity measurements. With respect to the His108 data, the fast phase of degradation observed between 3000 and 7000s is not simulated. The standard errors reported in Table 3.2 are a subject of "less than exact science"³³, as they often underestimate the true error. Nevertheless, their high values relative to the actual parameter values are another indication for the poor fit. Further fits were conducted with different initial estimates and constraints, but a combination of reasonable parameter values and a good fit could not be achieved.

We infer from these results that our model is too simple to simulate the ox-

idation kinetics of GAPDH in SRNOM-sensitized photolyses. It seems not justified to assume only two different conformational states of GAPDH with corresponding k_{rxn} and a constant denaturation rate transforming the population of GAPDH from one state to the other. Examining the data used here more deeply, it seems rather plausible that a short initial slow oxidation phase is followed by a fast oxidation phase between 2000 and 6000s before again a slow phase begins (Compare with Figure 3.4c). However, one has to be aware that such interpretations are based on data that shows considerable scatter.

Table 3.2: Parameters obtained from χ^2 fit

rate	value	std. error
r_{den}	$3.1 \times 10^{-4} \text{s}^{-1}$	$2.9 \times 10^{-3} \text{s}^{-1}$
$k_{rxn54,den}$	$1.74 \times 10^8 \text{M}^{-1} \text{s}^{-1}$	$9.43 \times 10^8 \text{M}^{-1} \text{s}^{-1}$
$k_{rxn108,den}$	$7.95 \times 10^7 \text{M}^{-1} \text{s}^{-1}$	$9.15 \times 10^7 \text{M}^{-1} \text{s}^{-1}$

4 Conclusion

The aim of this work was to elucidate the photodegradation of proteins in aquatic systems. To study this process, we followed a reductionist approach. Using a well-characterized model protein, GAPDH, and a well-defined system, we were able to assess $^1\text{O}_2$ reaction rate constants k_{rxn} of individual His residues within the native protein. In general, k_{rxn} showed a strong correlation with the $^1\text{O}_2$ -accessible surface area ($^1\text{O}_2$ -ASA) of the respective His residues. This led to the conclusion that the accessibility of a specific His residue is a main parameter in modulating the reactivity of these amino acids with $^1\text{O}_2$.

Knowing about this concept, we moved on to a more natural system where DOM was used as sensitizing compound for the production of $^1\text{O}_2$. We found that in these DOM-sensitized photolyses, values and ratio of k_{rxn} for the most exposed and most buried His residue in GAPDH have altered. Moreover, it was possible to follow these changes over the course of a DOM-sensitized photolysis. Whereas at the beginning of the experiment the k_{rxn} values had the same 3 to 4 fold difference as in native GAPDH, they might have equalized after two hours photolysis. Both observations indicate that the accessibilities of these residues changed over the course of DOM-sensitized photolyses, which implies that GAPDH underwent conformational changes.

We applied additional tools to further assess changes in the structure of GAPDH. Fluorescence studies following the Stokes

shift of GAPDH confirmed that the protein undergoes conformational changes when in solution with DOM. A significant Stokes shift was observed both in photolysed and dark DOM containing solutions, but in the former case the shift was more pronounced and faster than in the dark control. Control experiments showed that this shift was only small when the protein was in solutions without DOM and under the same conditions. We concluded from these results that interactions of GAPDH with DOM are the main cause for changes in the conformation of the protein.

These interactions can be either direct, via electrostatic and hydrophobic forces for example, or indirect via reactive species produced upon irradiation of DOM. Our data suggests that both types play a role. On one side, a significant spectral shift was observed in the dark, where no reactive species are present, indicating that the interaction or association of DOM with GAPDH contributes to the conformational change. On the other side, this Stokes shift was more pronounced in the SRNOM-sensitized photolysis than in the dark control experiment. This denotes that reactive species may further promote conformational changes and possibly lead to complete unfolding.

The interactions of proteins with natural organic matter are not well studied. Scientific literature often suggests that protein-organic matter interactions such as encapsulation may increase protein preservation, as it protects these biomolecules

from chemical or microbiological degradation.^{34,5,35} In contrast, we showed that these interactions may also lead to major conformational changes of a protein and an enhancement in its susceptibility to photo-oxidation.

The results obtained here are not generalizable. The kind of effect that natural organic matter has on proteins depends on the protein,³⁶ the type of organic matter, and external conditions such as pH, temperature or ionic strength.^{37,38} Our model protein GAPDH is not environmentally relevant and the DOM concentration applied here is high compared to aquatic systems.²¹ Nevertheless, this work illustrates a mechanism that needs to be taken into account when it comes to modelling both the fate of a specific protein as well as general N-cycling dynamics in sunlit waters.

Acknowledgments

You were the best supervisors I could imagine.
Thank you, Rachel and Kris.

References

1. Bronk, D. *Biogeochemistry of Marine Dissolved Organic Matter*. Academic Press, USA, (2002).
2. Billen, G. In *Microbial Enzymes in Aquatic Environments*, Chróst, R., editor, Brock/Springer Series in Contemporary Bioscience, 123–143. Springer New York (1991).
3. Keil, R. and Kirchman, D. *Limnology and Oceanography* **38**(6), 1256–1270 (1993).
4. Berman, T. and Bronk, D. *Aquatic Microbial Ecology* **31**(3), 279–305 (2003).
5. Nguyen, R. and Harvey, H. *Geochimica Et Cosmochimica Acta* **65**(9), 1467–1480 (2001).
6. Rillig, M., Caldwell, B., Wösten, H., and Sollins, P. *Biogeochemistry* **85**(1), 25–44 (2007).
7. Amelung, W., Zhang, X., and Flach, K. *Geoderma* **130**, 207 – 217 (2006).
8. Armengaud, J., Christie-Oleza, J. A., Clair, G., Malard, V., and Duport, C. *Expert Review of Proteomics* **9**(5), 561–575 (2012).
9. Tranvik, L., Sherr, E., and Sherr, B. *Marine Ecology Progress Series* **92**(3), 301–309 (1993).
10. Davies, M. *Biochimica et Biophysica Acta - Proteins and Proteomics* **1703**(2), 93–109 (2005).
11. Pattison, D. I., Rahmanto, A. S., and Davies, M. J. *Photochem. Photobiol. Sci.* **11**, 38–53 (2012).
12. Wilkinson, F., Helman, W., and Ross, A. *Journal of Physical and Chemical Reference Data* **24**(2), 663–1021 (1995).
13. Kim, J., Rodriguez, M. E., Guo, M., Kenney, M. E., Oleinick, N. L., and Anderson, V. E. *Free Radical Biology and Medicine* **44**(9), 1700–1711 (2008).
14. Wigginton, K. R., Menin, L., Montoya, J. P., and Kohn, T. *Environmental Science & Technology* **44**(14), 5437–5443 (2010).
15. Michaeli, A. and Feitelson, J. *Photochemistry and Photobiology* **65**(2), 309–315 (1997).

16. Jensen, R. L., Arnbjerg, J., and Ogilby, P. R. *Journal of the American Chemical Society* **134**(23), 9820–9826 (2012).
17. Pettersen, E., Goddard, T., Huang, C., Couch, G., Greenblatt, D., Meng, E., and Ferrin, T. *Journal of Computational Chemistry* **25**(13), 1605–1612 (2004).
18. Cowan-Jacob, S., Kaufmann, M., Anselmo, A., Stark, W., and Grutter, M. *Acta Crystallographica Section D-Biological Crystallography* **59**(Part 12), 2218–2227 (2003).
19. Fraczkiewicz, R. and Braun, W. *Journal of Computational Chemistry* **19**(3), 319–333 (1998).
20. Wershaw, R. *Soil Science* **164**(11), 803–813 (1999).
21. Schwarzenbach, R. P., Gschwend, P. M., and Imboden, D. M. *Environmental Organic Chemistry*. John Wiley & Sons, Inc, Hoboken, New Jersey, (2003).
22. Haag, W. and Hoigne, J. *Environmental Science & Technology* **20**(4), 341–348 (1986).
23. Haag, W. and Hoigne, J. *Chemosphere* **14**(11-12), 1659–1671 (1985).
24. Latch, D. and McNeill, K. *Science* **311**(5768), 1743–1747 (2006).
25. Boreen, A. L., Edhlund, B. L., Cotner, J. B., and McNeill, K. *Environmental Science & Technology* **42**(15), 5492–5498 (2008).
26. Latch, D., Stender, B., Packer, J., Arnold, W., and McNeill, K. *Environmental Science & Technology* **37**(15), 3342–3350 (2003).
27. Greenwood, N.N.; Earnshaw, A. *Chemistry of the Elements*. Pergamon Press, (1984).
28. Eftink, M. *Methods of Biochemical Analysis* **35**, 127–205 (1991).
29. Lundeen, R. and McNeill, K. *not published yet* , (2013).
30. He, R., Li, Y., Wu, X., and Li, L. *Biochimica et Biophysica Acta - Protein Structure and Molecular Enzymology* **1253**(1), 47–56 (1995).
31. Savitzky, A. and Golay, M. J. E. *Analytical Chemistry* **36**(8), 1627–1639 (1964).
32. Lee, H., Howell, S., Sanford, R., and Beisswenger, P. In *Maillard Reaction: Chemistry at the Interface of Nutrition, Aging, and Disease*, Baynes, JW and Monnier, VM and Ames, JM and Thorpe, SR, editor, volume 1043 of *Annals of the New York Academy of Sciences*, 135–145. New York Acad Sciences, (2005).
33. Johnson, K. A. In *Methods in Enzymology*, Brand, M. L. J. L., editor, volume 467 of *Methods in Enzymology*, 601 – 626. Academic Press (2009).

34. Zang, X., van Heemst, J., Dria, K., and Hatcher, P. *Organic Chemistry* **31**(7-8), 679–695 (2000).
35. Tomaszewski, J. E., Schwarzenbach, R. P., and Sander, M. *Environmental Science & Technology* **45**(14), 6003–6010 (2011).
36. Morales-Belpaire, I. and Gerin, P. A. *Protein Journal* **31**(1), 84–92 (2012).
37. Tan, W. F., Koopal, L. K., Weng, L. P., van Riemsdijk, W. H., and Norde, W. *Geochimica Et Cosmochimica Acta* **72**(8), 2090–2099 (2008).
38. Tan, W. F., Koopal, L. K., and Norde, W. *Environmental Science & Technology* **43**(3), 591–596 (2009).

Appendix

Direct photolysis - Control for direct photodegradation

To control for direct photodegradation, an experiment was conducted where GAPDH was irradiated in AmBic without added sensitizer. The same light conditions as in SRNOM-sensitized photolyses were applied ($\lambda = 400\text{nm}$ cut off filter, high light intensity). Time points sampled were 0min, 1h 30min, 3h 10min, 4h 30min 6h 20min and 7h 30min; whereas for the first time point (t_0) and last time point (t_6) three aliquots were analysed, only one aliquot was taken for the other four time points.

Measured intensities were corrected as described before and normalized to the average intensity of t_0 . These normalized intensities of tryptic peptides containing His54 and His108 (their two most intense charge states) are shown in Figure A.1. In general, the highest peptide intensities are found in t_0 aliquots. However, with the exception of "53-58 His54 [$Z=2$]", one of the three aliquots of t_0 has an intensity that is comparable to the intensities of other time points. All other time points show equal intensities and no trend is observable.

An unpaired t-test for differences between two normal distributed populations with equal but unknown variance was conducted to test the hypothesis, that aliquots of t_6 ($27'000\text{s} = 7.5\text{h}$) had significantly lower (corrected) mean intensities than aliquots of t_0 (one-sided test). With a significance level of 0.95 and 4 degrees of freedom, the null hypothesis (H_0 , same intensity mean) is rejected if $T > 2.354$. The test failed to reject H_0 for all but one His peptide m/z value, "53-58 His54 [$Z=2$]",. Therefore, no significant difference in the intensity means of t_0 and t_6 could be detected for most peptide m/z values.

Unpaired-t-test for differences of two normal distributed samples with equal but unknown variance

t (p=0.95; df=4; one-sided) = 2.354

His54 peptides*	t_0				t_6				n1	n2	T			
	0	0	0		5400	11400	16200	22800				27000	27000	27000
53-58_Hext[Z=1]	1066426	739984	1267851		872308	587862	531296	676812	741813	964815	435785	3	3	1.430198
53-58_Hext[Z=2]	2573650	2637286	3173801		1664445	1640351	1583266	1398534	1428660	2227737	1082103	3	3	3.124795
Sum	3640075	3377269	4441652		2536753	2228212	2114561	2075346	2170474	3192552	1517888	3	3	2.61722
Average Z=1	1024754								714138					
Average Z=2	2794912								1579500					
STD Z=1	266390								265599					
STD Z=2	329666								587523					
Average Sum	3819666								2203638					
STD Sum	554452								844098					

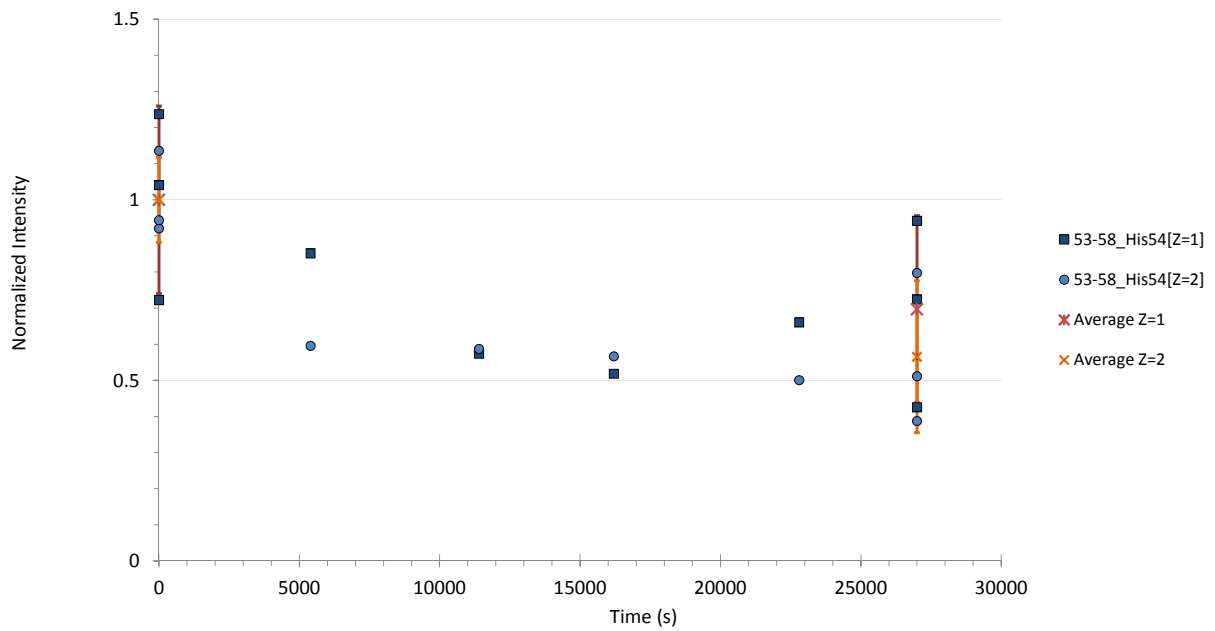
H_0 not rejected = same population mean
 H_0 rejected = not same population mean

Unpaired-t-test for differences of two normal distributed samples with equal but unknown variance

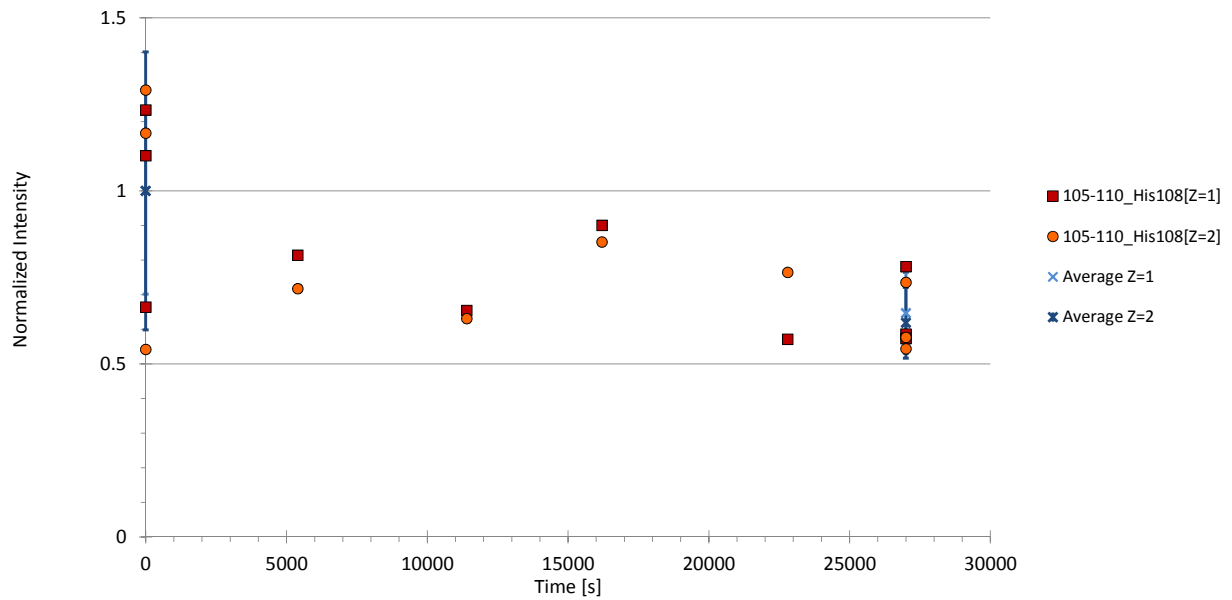
His108 peptides*	t_0				t_6				n1	n2	T			
	0	0	0		5400	11400	16200	22800				27000	27000	27000
105-110_Hint[Z=1]	1308078	782263	1464802		966127	776854	1068668	677944	695715	680658	927558	3	3	1.90902
105-110_Hint[Z=2]	1890127	793085	1707778		1050050	923692	1247437	1118785	844258	795721	1076643	3	3	1.593304
Sum	3198205	1581348	3172580		2016177	1700547	2316105	1796730	1539973	1476379	2004201	3	3	1.74495
Average Z=1	1187047								767977					
Average Z=2	1463664								905541					
STD Z=1	354136								138406					
STD Z=2	587851								150153					
Average Sum	2650711								1673518					
STD Sum	926184								288140					

H_0 not rejected = same population mean
 H_0 rejected = not same population mean

* corrected by internal standard peptides 18-24 [$Z=1,2$] and 184-191 [$Z=1,2$]



(a) Normalized intensities of peptides containing His54.



(b) Normalized intensities of peptides containing His108.

Figure A.1: Test for direct photodegradation of peptides containing His54 and His108 from tryptic digestion of GAPDH. Intensities are corrected by internal standard peptide m/z values (18-24 [Z=1,2] and 184-191 [Z=1,2]) and normalized to the average intensity of t_0 aliquots. Although two t_0 aliquots usually show higher intensities than other aliquots, no significant difference between t_0 and t_6 mean intensities was found on a significance level of 0.95. An exception to this is "53-58 His54 [Z=2]".

Examining why corrected His peptide intensities in two t_0 aliquots are usually higher than in all other samples, we found that the measured, uncorrected His peptide intensities were *per se* not higher than those of other time points. However, in those two t_0 aliquots, one of the peptides (18-24, Z=1,2) that served as internal standards had 3.5 to 30 times lower intensities than in the third t_0 aliquot. No comparable behaviour was found for any other tryptic peptide m/z value. We concluded that these internal standard peptide m/z values intensities were determined incorrectly for two t_0 aliquots. This lowered the correction factor (CF) drastically and thereby increased the "corrected" His peptide intensities of the affected aliquots. Therefore, we excluded these two internal standard peptide m/z values (18-24, Z=1,2) from CF calculation. Newly corrected His peptide intensities are shown in Figure A.2. The plots show scattering intensities, but no general trend or differences between t_0 and other time points. Applying the same statistical test as before, no significant difference in mean intensities of t_0 and t_6 aliquots can be found for all His peptide m/z values.

Consequently, we find no direct photodegradation of His peptides of interest under the light conditions used for SRNOM-sensitized photolyses. However, given the high variance of both the t_0 and the t_6 intensities, the maximally possible direct photodegradation rates of His peptide m/z values that are not excludable with this control experiment are in the same order of magnitude as the observed $^1\text{O}_2$ oxidation rates (see below). Although we don't expect direct photodegradation to occur or account for a significant share on our observed degradation rates, a better planned and differently conducted experiment is needed to confirm this assumption. Another possibility might be to infer maximum direct oxidation rates for His containing peptides from the degradation rates of peptides containing amino acids that are more prone to undergo direct oxidation (Trp, Tyr, and Phe).

Unpaired-t-test for differences of two normal distributed samples with equal but unknown variance

t (p=0.95; df=4; one-sided) = 2.354

His54 peptides*				t_0				t_6						
time (s)	0	0	0	5400	11400	16200	22800	27000	27000	27000	n1	n2	T	
53-58_Hext[Z=1]	1146939	1746117	1711749	2221385	1390098	943588	1625730	2053548	2496202	984449	3	3	-0.63358	
53-58_Hext[Z=2]	2767955	6223122	4285005	4238610	3878885	2811900	3359335	3954934	5763673	2444500	3	3	0.267718	
Sum	3914894	7969238	5996754	6459995	5268983	3755488	4985065	6008483	8259874	3428949	3	3	0.033595	
Average Z=1	1534935							Average Z=1	1844733					
Average Z=2	4425361							Average Z=2	4054369					
STD Z=1	336453							STD Z=1	777208					
STD Z=2	1731854							STD Z=2	1661819					
Average Sum	5960295							Average Sum	5899102					
STD Sum	2027418							STD Sum	2417319					

HO not rejected = same population mean
 HO rejected = not same population mean

t (p=0.95; df=4; one-sided) = 2.354

His108 peptides*				t_0				t_6						
time (s)	0	0	0	5400	11400	16200	22800	27000	27000	27000	n1	n2	T	
105-110_Hint[Z=1]	1406835	1860039	1977655	2460300	1837002	1897968	1628450	1925935	1761021	2095377	3	3	-0.90088	
105-110_Hint[Z=2]	2032828	1871419	2305702	2674016	2184226	2215464	2687367	2337143	2058715	2432165	3	3	-1.21786	
Sum	3439663	3731458	4283357	5134316	4021228	4113432	4315817	4263078	3819736	4527542	3	3	-1.19569	
Average Z=1	1748176							Average Z=1	1927444					
Average Z=2	2069983							Average Z=2	2276008					
STD Z=1	301403							STD Z=1	167183					
STD Z=2	219513							STD Z=2	194086					
Average Sum	3818159							Average Sum	4203452					
STD Sum	428477							STD Sum	357650					

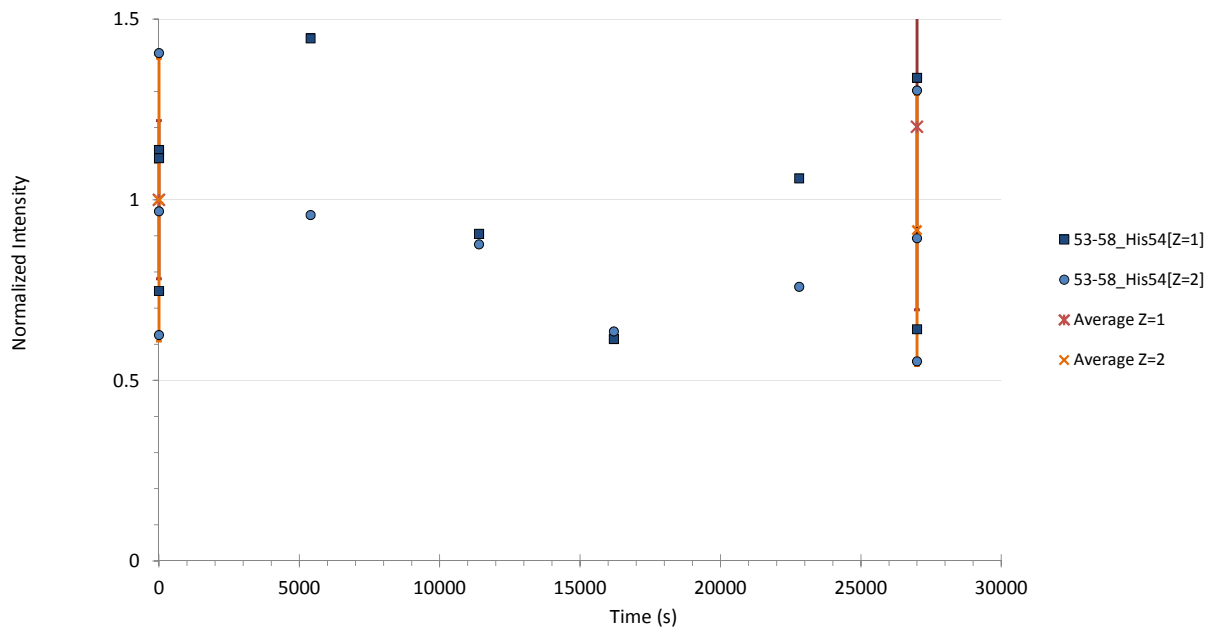
HO not rejected = same population mean
 HO rejected = not same population mean

* corrected by internal standard peptides 184-191 [Z=1,2] only

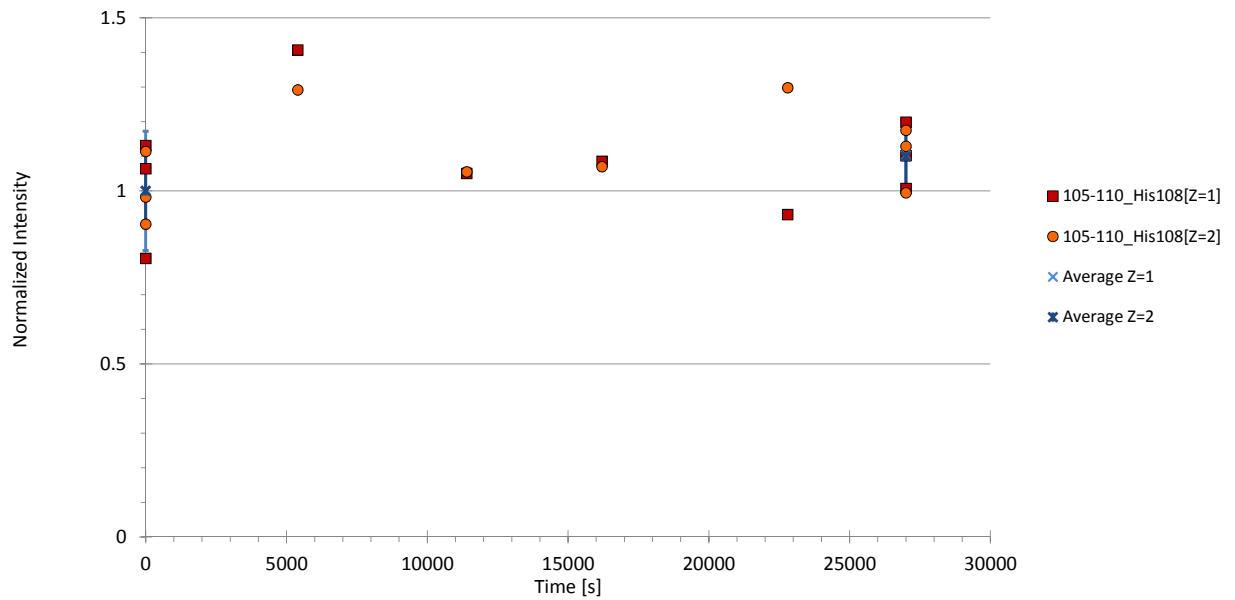
Maximum possible direct photodegradation with this test:

(Intensities corrected only with internal standard peptide 184-191):

p=0.95	AVE. t_0	STD	n	AV t_6	STD	n	T value	ln(T_6/T_0)	Maximum degradation rate		
									Equals a k_{rxn}	($[O_2]_{ss} = 8E-13$)	
	53-58_Hext[Z=1]	1534935	336453	3	383917	777208	3	2.354	-1.386	-5.13E-05 s ⁻¹	-6.42E+07 M ⁻¹ s ⁻¹
	53-58_Hext[Z=2]	4425361	1731854	3	1163290	1661819	3	2.354	-1.336	-4.95E-05 s ⁻¹	-6.19E+07 M ⁻¹ s ⁻¹
	105-110_Hint[Z=1]	1748176	301403	3	1279748	167183	3	2.354	-0.312	-1.16E-05 s ⁻¹	-1.44E+07 M ⁻¹ s ⁻¹
	105-110_Hint[Z=2]	2069983	219513	3	1671758	194086	3	2.354	-0.214	-7.91E-06 s ⁻¹	-9.89E+06 M ⁻¹ s ⁻¹



(a) Test for direct photodegradation of peptides containing His54.



(b) Test for direct photodegradation of peptides containing His108.

Figure A.2: Test for direct photodegradation of peptides containing His54 and His108 from tryptic digestion of GAPDH. Intensities are corrected by internal standard peptide 184-191 ($Z=1,2$) only and normalized to the average intensity of t_0 aliquots.

Derivation of the formula used in section 3.2

We assume that both His residues are oxidized by 1O_2 according to a pseudo-first order kinetic:

$$\frac{d[His_{54}]}{dt} = -k_{rxn,His54} * [^1O_2] * [His_{54}]$$

and

$$\frac{d[His_{108}]}{dt} = -k_{rxn,His108} * [^1O_2] * [His_{108}]$$

Neglecting for the moment that the reaction rate constants k_{rxn} are themselves time dependent, this leads to the antiderivatives:

$$[His_{54}]_t = [His_{54}]_0 * e^{-k_{rxn,His54} * [^1O_2] * t}$$

and

$$[His_{108}]_t = [His_{108}]_0 * e^{-(k_{rxn,His108}) * [^1O_2] * t}$$

The ratio of the normalized peptide intensities therefore follows:

$$\frac{([His_{108}]_t/[His_{108}]_0)}{([His_{54}]_t/[His_{54}]_0)} = e^{(k_{rxn,His54} - k_{rxn,His108}) * [^1O_2] * t}$$

which leads to

$$\ln\left(\frac{([His_{108}]_t/[His_{108}]_0)}{([His_{54}]_t/[His_{54}]_0)}\right) = (k_{rxn,His54} - k_{rxn,His108}) * [^1O_2] * t$$

Differentiating with respect to the 1O_2 -dose ($[^1O_2] * t$), again neglecting that k_{rxn} are time dependent, yields:

$$\frac{d(\ln(\frac{[His_{108}]_t}{[His_{108}]_0}) - \ln(\frac{[His_{54}]_t}{[His_{54}]_0}))}{d(t * [^1O_2])} = k_{rxn,His54} - k_{rxn,His108}$$

Replacing k_{rxn} with $k_{rxn}(t)$ we finally get:

$$\frac{d(\ln(\frac{[His_{108}]_t}{[His_{108}]_0}) - \ln(\frac{[His_{54}]_t}{[His_{54}]_0}))}{d(t * [^1O_2])} = k_{rxn,His54}(t) - k_{rxn,His108}(t)$$

Note: As we assume $[^1O_2]$ to be constant, we can omit the integration and differentiation steps by making use of:

$$\frac{\frac{d[His_{xy}]}{dt}}{[His_{xy}]} = \frac{\frac{d[His_{xy}]}{[His_{xy}]}}{dt} = \frac{d(\ln[His_{xy}])}{dt}$$

MB-sensitized photolysis fluorescence study

An experiment was conducted by Rachel Lundeen to check for denaturation of GAPDH during photolysis with MB. The photolysis was carried out for 35min; 300 μ l aliquots were removed at different time points and immediately measured. The excitation wavelength was 295nm to minimize Tyr interference. A blank sample of 10 μ M MB and AmBic buffer was analyzed and used for background correction. The results are shown in Figure A.3.

Over the course of the photolysis, fluorescence intensity decreased as Trp residues were degraded. However, the maximum emission wavelength was always between 337-340nm, indicating that no denaturation occurred.

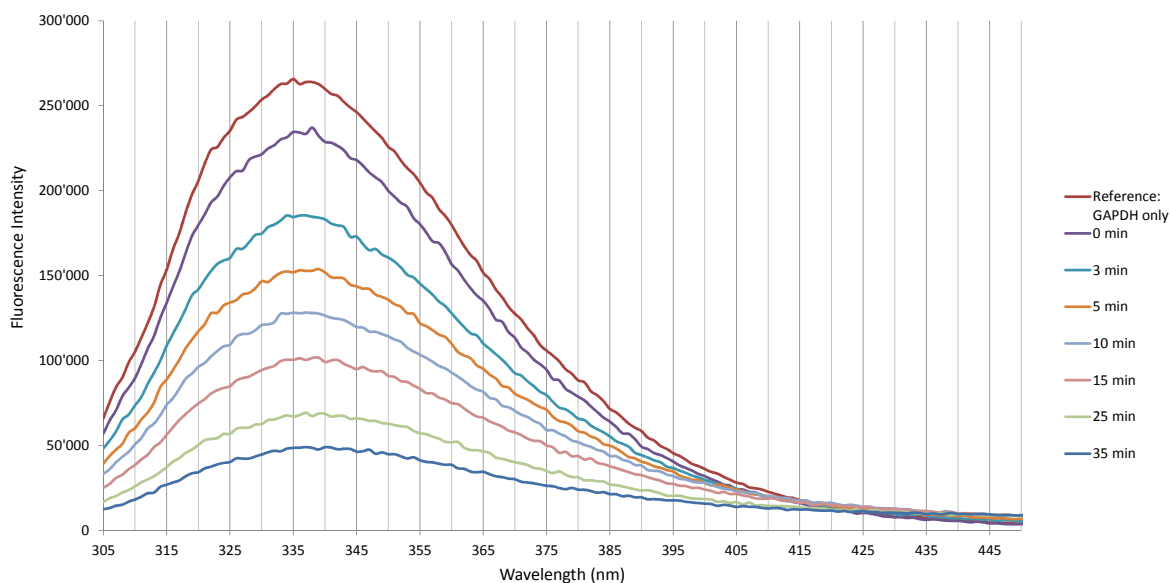


Figure A.3: Fluorescence emission spectra of GAPDH over the course of a MB-sensitized photolysis. Excitation wavelength was 295nm. Figure with kind permission of Rachel Lundeen.

Fluorescence spectra of denatured GAPDH

To determine fluorescence emission maxima of native and fully denatured GAPDH, we measured the fluorescence emission spectra of GAPDH in solution with different concentrations of Guanidine Hydrochloride (GndHCl). GAPDH was dissolved in AmBic buffer in LoBind Eppendorf tubes and the appropriate amount of GndHCl was added. End concentrations of GAPDH were $1.5\mu\text{M}$. The solution was slightly vortexed, let stand for 2.5h in the dark, and measured as described before.

Figure A.4 shows the fluorescence emission spectra upon excitation with 280nm. Native GAPDH (0M GndHCl) has its emission peak at 337nm. The emission maximum red-shifts with increasing GndHCl concentrations and reaches 354nm at 1.5M and 2M GndHCl. Fluorescence intensity increases first, but decreases again. An interpretation of this spectral changes is given in He et al. (1995)³⁰.

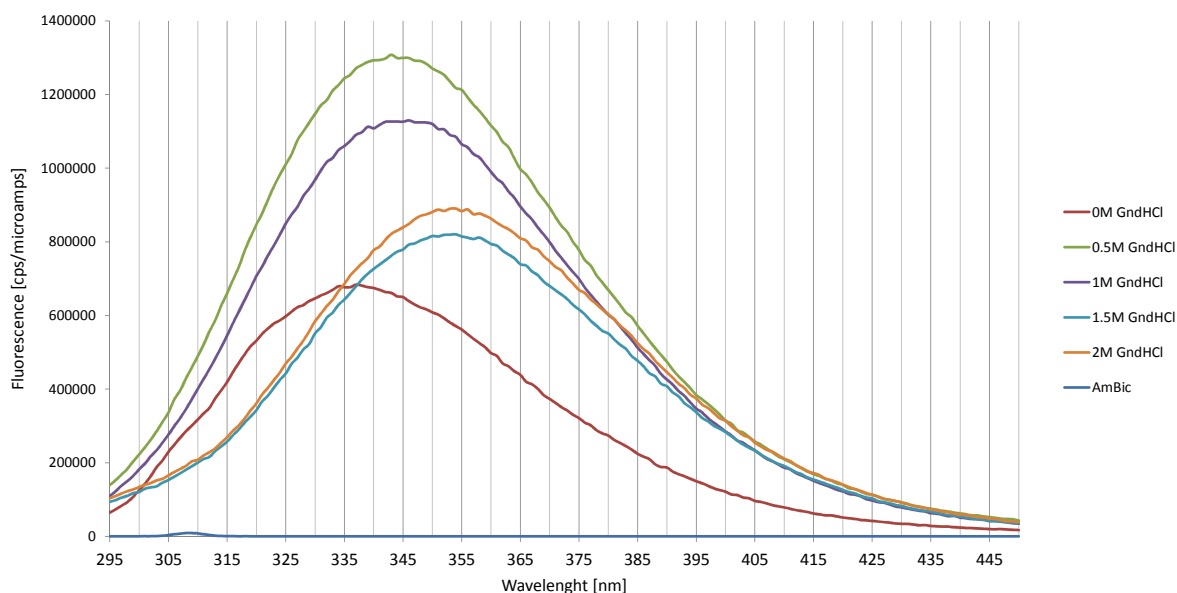


Figure A.4: Fluorescence emission spectra of GAPDH in solution with different concentrations of GndHCl. Excitation wavelength was 280nm. Native GAPDH has its fluorescence emission peak at 337nm, whereas the fluorescence maxima of fully denatured GAPDH is at 354nm.

Absorbance spectra of SRNOM

An absorbance spectrum of a 50mgC/l SRNOM solution was recorded on a Cary 300 Bio UV-Visible Spectrophotometer (Varian, USA). The solution was placed in an quartz cuvette (Hellma Analytics, Germany) with a light path length of 10mm, slit width was 2nm. The spectrum is shown in Figure A.5 together with the estimated corresponding absorbance spectrum for a microcuvette like the ones used in the fluorescence studies. The only correction applied between the two spectra was the light path length; differences in glass types and widths were neglected. The spectra for the microcuvette is therefore only a rough estimate, but is sufficient to show that the gradient in absorbance between 320nm and 370nm is not strong enough to manipulate fluorescence emission peak positions by inner filter effects.

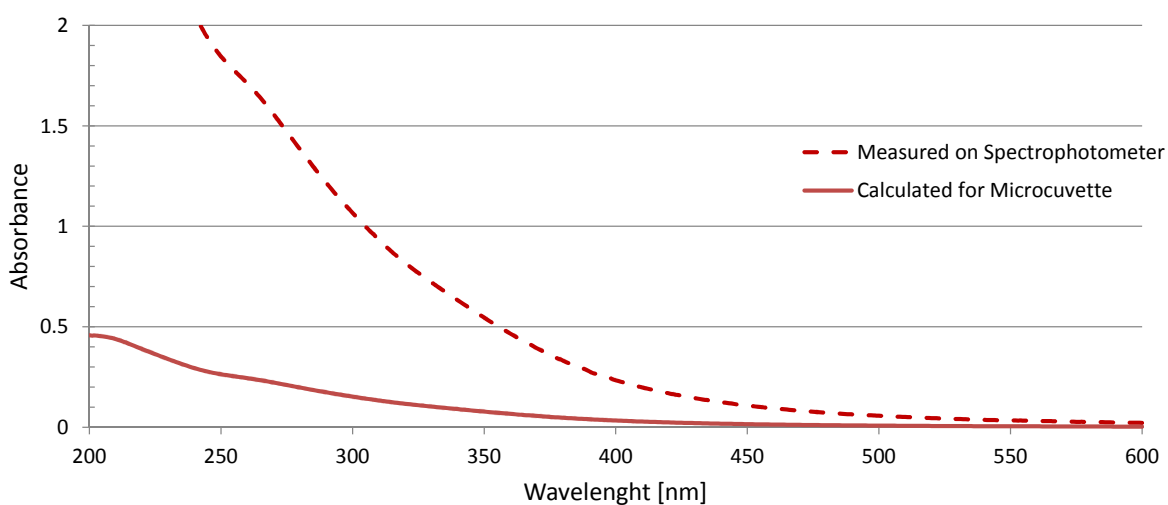


Figure A.5: Absorbance spectra of a solution with 50mgC/l SRNOM as measured in a spectrophotometer and calculated for a microcuvette. The latter spectrum is only a rough estimate, based on a comparison of the different light path lengths.

Photolysis data

Table A.1: Linearized degradation rates of His containing peptides, observed $^1\text{O}_2$ concentrations and calculated k_{rxn} for all photolyses.

Peptide	linear regression of linearized corrected intensities				norm. weight	average slope [s ⁻¹]	std. error [s ⁻¹]	k_{rxn} [M ⁻¹ s ⁻¹]	std. error [M ⁻¹ s ⁻¹]
	slope [s ⁻¹]	std. dev [s ⁻¹]	R ²						
MB-sensitized photolysis		Observed singlet oxygen concentration [¹ O ₂] _{ss} :			7.23 (+/- 0.33) E-11 M				
53-58_His54[Z=1]	-3.74E-03	4.19E-04	0.97	0.13					
53-58_His54[Z=2]	-4.45E-03	5.01E-04	0.97	0.78	4.37E-03	4.35E-04	6.05E+07	6.60E+06	
53-58_His54[Z=3]	-4.66E-03	2.05E-03	0.82	0.09					
105-110_His108[Z=1]	-1.55E-03	1.21E-04	0.98	0.29					
105-110_His108[Z=2]	-1.39E-03	8.63E-05	0.98	0.69	1.44E-03	6.87E-05	1.99E+07	1.31E+06	
105-110_His108[Z=3]	-1.34E-03	1.57E-04	0.96	0.03					
115-136_His134[Z=2]	-1.80E-03	9.02E-04	0.70	0.00					
115-136_His134[Z=3]	-2.69E-03	4.19E-04	0.94	0.05	2.06E-03	2.63E-04	2.85E+07	3.85E+06	
115-136_His134[Z=4]	-2.82E-03	3.98E-04	0.95	0.09					
116-136_His134[Z=2]	-1.45E-03	-2.50E-03	0.89	0.05					
116-136_His134[Z=3]	-1.93E-03	2.92E-04	0.91	0.76					
116-136_His134[Z=4]	-2.85E-03	2.98E-04	0.97	0.04					
321-331_His327[Z=2]	-1.81E-03	1.41E-04	0.98	0.05					
321-331_His327[Z=3]	-1.74E-03	1.63E-04	0.97	0.19	1.60E-03	1.06E-04	2.21E+07	1.77E+06	
321-332_His327[Z=1]	-1.94E-03	6.27E-04	0.82	0.01					
321-332_His327[Z=2]	-1.69E-03	1.74E-04	0.96	0.18					
321-332_His327[Z=3]	-1.50E-03	1.67E-04	0.95	0.58					
SRNOM-sensitized photolysis I		Observed singlet oxygen concentration [¹ O ₂] _{ss} :			5.84(+/-0.20)E-13 M				
53-58_His54[Z=1]	-4.41E-05	5.31E-06	0.90	0.27					
53-58_His54[Z=2]	-4.06E-05	4.12E-06	0.92	0.64	-4.13E-05	3.13E-06	7.54E+07	6.35E+06	
53-58_His54[Z=3]	-3.82E-05	9.95E-06	0.65	0.09					
105-110_His108[Z=1]	-3.87E-05	4.85E-06	0.89	0.49					
105-110_His108[Z=2]	-2.89E-05	4.30E-06	0.85	0.48	-3.35E-05	3.17E-06	6.12E+07	6.20E+06	
105-110_His108[Z=3]	-2.14E-05	8.03E-06	0.47	0.03					
SRNOM-sensitized photolysis II		Observed singlet oxygen concentration [¹ O ₂] _{ss} :			7.77(+/-0.29)E-13 M				
53-58_His54[Z=1]	-8.05E-05	5.85E-06	0.96	0.28					
53-58_His54[Z=2]	-7.32E-05	3.80E-06	0.98	0.68	-7.54E-05	3.07E-06	9.71E+07	5.36E+06	
53-58_His54[Z=3]	-7.83E-05	8.33E-06	0.92	0.04					
105-110_His108[Z=1]	-5.29E-05	7.43E-06	0.86	0.50					
105-110_His108[Z=2]	-5.29E-05	5.22E-06	0.93	0.50	-5.31E-05	4.51E-06	6.84E+07	6.34E+06	
105-110_His108[Z=3]	-8.91E-05	0.00E+00		0.01					
SRNOM-sensitized photolysis III		Observed singlet oxygen concentration [¹ O ₂] _{ss} :			7.89(+/-0.20)E-13 M				
53-58_His54[Z=1]	-6.36E-05	6.89E-06	0.89	0.27					
53-58_His54[Z=2]	-6.20E-05	5.56E-06	0.92	0.70	-6.27E-05	4.30E-06	7.95E+07	5.81E+06	
53-58_His54[Z=3]	-6.99E-05	5.81E-06	0.91	0.04					
105-110_His108[Z=1]	-4.79E-05	5.07E-06	0.89	0.50					
105-110_His108[Z=2]	-4.52E-05	3.96E-06	0.92	0.49	-4.66E-05	3.21E-06	5.90E+07	4.33E+06	
105-110_His108[Z=3]	-4.75E-05	4.09E-06	0.92	0.01					

Accessibilities of His residues

Table A.2: $^1\text{O}_2$ -Accessible surface areas ($^1\text{O}_2$ -ASA) of all His residues in GAPDH as calculated by Getarea¹⁹. Average values for His residue sidechains were used in this work.

<u>Sidechain</u> <u>Residue</u> <u>$^1\text{O}_2$-ASA</u>	<u>Chain</u>				<u>Sidechain</u>
<u>Residue</u>	<u>Q</u>	<u>P</u> (NAD+bound)	<u>Q</u>	<u>R</u> (NAD+bound)	<u>Residue Average</u>
His 38	107.56	106.5	111.73	107.98	108.44
His 50	1.65	1.73	1.88	1.67	1.73
His 54	131.27	144.66	132.3	143.06	137.82
His 108	0.16	0.21	0.31	0.16	0.21
His 134	35.72	34.26	33.71	34.49	34.55
His 162	29.69	30.33	20.31	30.27	27.65
His 164	59.77	71.18	71.14	71.31	68.35
His 176	32.88	31.26	28.66	27.01	29.95
His 288	52.54	52.45	52.32	53.03	52.59
His 303	71.98	79.26	77.73	71.68	75.16
His 327	21.19	20.25	22.95	20.38	21.19

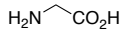
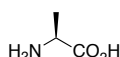
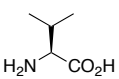
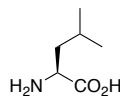
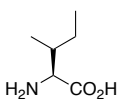
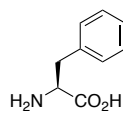
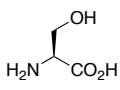
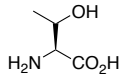
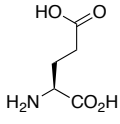
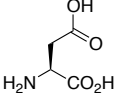
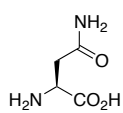
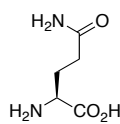
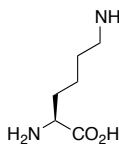
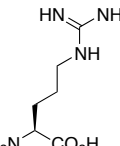
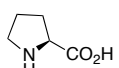
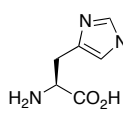
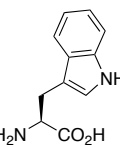
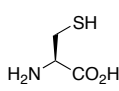
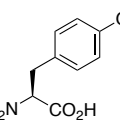
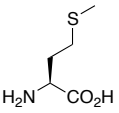
 <p>Glycine (Gly; G)</p>	 <p>Alanine (Ala; A)</p>	 <p>Valine (Val; V)</p>	 <p>Leucine (Leu; L)</p>	 <p>Isoleucine (Ile; I)</p>
 <p>Phenylalanine (Phe; F)</p>	 <p>Serine (Ser; S)</p>	 <p>Threonine (Thr; T)</p>	 <p>Glutamic Acid (Glu; E)</p>	 <p>Aspartic Acid (Asp; D)</p>
 <p>Asparagine (Asn; N)</p>	 <p>Glutamine (Gln; Q)</p>	 <p>Lysine (Lys; K)</p>	 <p>Arginine (Arg; R)</p>	 <p>Proline (Pro; P)</p>
 <p>Histidine (His; H) Photooxidizable</p>	 <p>Tryptophan (Trp; W) Photooxidizable</p>	 <p>Cysteine (Cys; C) Photooxidizable</p>	 <p>Tyrosine (Tyr; Y) Photooxidizable</p>	 <p>Methionine (Met; M) Photooxidizable</p>

Figure A.7: Structure and abbreviations of all proteinogenic amino acids. Photo-oxidizable amino acids are in the bottom row. With kind permission of Rachel Lundeen.

Table A.3: Monoisotopic masses and expected m/z values for predicted peptides after tryptic digestion.

GAPDH Trypsin Digestion		MS Charge	Monoisotopic	Peptide Sequence	Sequence	Missed
Name	Expected m/z	(Z)	Mass		Position	Cleavage
1-10*[Z=1]	1032.594	+1	1031.587	VK_VGVNGFGR ¹⁰	001-010	1
1-10*[Z=2]	516.801	+2	1031.587	VK_VGVNGFGR ¹⁰	001-010	1
1-10*[Z=3]	344.87	+3	1031.588	VK_VGVNGFGR ¹⁰	001-010	1
3-10[Z=1]	805.431	+1	804.424	GVNGFGR ¹⁰	003-010	0
3-10[Z=2]	403.219	+2	804.423	GVNGFGR ¹⁰	003-010	0
14-17[Z=1]	488.318	+1	487.311	LVTR	014-017	0
14-17[Z=2]	244.663	+2	487.311	LVTR	014-017	0
18-24[Z=1]	694.351	+1	693.344	AAF ²⁰ NSGK	018-024	0
18-24[Z=2]	347.679	+2	693.343	AAF ²⁰ NSGK	018-024	0
18-52*_H38H50[Z=3]	1331.638	+3	3991.892	AAF ²⁰ NSGK_VDVVAI ³⁰ NDPFIDLHYM ⁴⁰ VYMFQYDSTH ⁵⁰ GK	018-052	1
18-52*_H38H50[Z=4]	998.98	+4	3991.891	AAF ²⁰ NSGK_VDVVAI ³⁰ NDPFIDLHYM ⁴⁰ VYMFQYDSTH ⁵⁰ GK	018-052	1
18-52*_H38H50[Z=5]	799.386	+5	3991.894	AAF ²⁰ NSGK_VDVVAI ³⁰ NDPFIDLHYM ⁴⁰ VYMFQYDSTH ⁵⁰ GK	018-052	1
18-52*_H38H50[Z=6]	666.322	+6	3991.888	AAF ²⁰ NSGK_VDVVAI ³⁰ NDPFIDLHYM ⁴⁰ VYMFQYDSTH ⁵⁰ GK	018-052	1
25-52_H38H50[Z=2]	1659.286	+2	3316.557	VDVVAI ³⁰ NDPFIDLHYM ⁴⁰ VYMFQYDSTH ⁵⁰ GK	025-052	0
25-52_H38H50[Z=3]	1106.526	+3	3316.556	VDVVAI ³⁰ NDPFIDLHYM ⁴⁰ VYMFQYDSTH ⁵⁰ GK	025-052	0
25-52_H38H50[Z=4]	830.147	+4	3316.559	VDVVAI ³⁰ NDPFIDLHYM ⁴⁰ VYMFQYDSTH ⁵⁰ GK	025-052	0
25-52_H38H50[Z=5]	664.319	+5	3316.559	VDVVAI ³⁰ NDPFIDLHYM ⁴⁰ VYMFQYDSTH ⁵⁰ GK	025-052	0
53-58_H54[Z=1]	688.377	+1	687.370	FHGTVK	053-058	0
53-58_H54[Z=2]	344.692	+2	687.369	FHGTVK	053-058	0
53-58_H54[Z=3]	230.131	+3	687.371	FHGTVK	053-058	0
53-63*_H54[Z=1]	1187.616	+1	1186.609	FHGTVK_AE ⁶⁰ NGK	053-063	1
53-63*_H54[Z=2]	594.312	+2	1186.609	FHGTVK_AE ⁶⁰ NGK	053-063	1
59-63[Z=1]	518.256	+1	517.249	AE ⁶⁰ NGK	059-063	0
59-63[Z=2]	259.632	+2	517.249	AE ⁶⁰ NGK	059-063	0
59-69*[Z=1]	1142.652	+1	1141.645	AE ⁶⁰ NGK_LVINGK	059-069	1
59-69*[Z=2]	571.83	+2	1141.645	AE ⁶⁰ NGK_LVINGK	059-069	1
59-69*[Z=3]	381.556	+3	1141.646	AE ⁶⁰ NGK_LVINGK	059-069	1
64-69[Z=1]	643.413	+1	642.406	LVINGK	064-069	0
64-69[Z=2]	322.21	+2	642.405	LVINGK	064-069	0
70-77[Z=1]	977.541	+1	976.534	A ⁷⁰ ITIFQER	070-077	0
70-77[Z=2]	489.274	+2	976.533	A ⁷⁰ ITIFQER	070-077	0
70-77[Z=3]	326.519	+3	976.535	A ⁷⁰ ITIFQER	070-077	0
70-83*[Z=1]	1615.879	+1	1614.872	A ⁷⁰ ITIFQER_DPA ⁸⁰ NIK	070-083	1
70-83*[Z=2]	808.443	+2	1614.871	A ⁷⁰ ITIFQER_DPA ⁸⁰ NIK	070-083	1
70-83*[Z=3]	539.298	+3	1614.872	A ⁷⁰ ITIFQER_DPA ⁸⁰ NIK	070-083	1
70-83*[Z=4]	404.725	+4	1614.871	A ⁷⁰ ITIFQER_DPA ⁸⁰ NIK	070-083	1
78-83[Z=1]	657.356	+1	656.349	DPA ⁸⁰ NIK	078-083	0
78-83[Z=2]	329.182	+2	656.349	DPA ⁸⁰ NIK	078-083	0
105-110_H108[Z=1]	596.351	+1	595.344	AGAHLK ¹¹⁰	105-110	0
105-110_H108[Z=2]	298.679	+2	595.343	AGAHLK ¹¹⁰	105-110	0
105-110_H108[Z=3]	199.455	+3	595.343	AGAHLK ¹¹⁰	105-110	0
115-136*_H134[Z=2]	1185.109	+2	2368.203	R_VIISA ¹²⁰ PSADAPMFVM ¹³⁰ GVNHEK	115-136	1
115-136*_H134[Z=3]	790.408	+3	2368.202	R_VIISA ¹²⁰ PSADAPMFVM ¹³⁰ GVNHEK	115-136	1
115-136*_H134[Z=4]	593.058	+4	2368.203	R_VIISA ¹²⁰ PSADAPMFVM ¹³⁰ GVNHEK	115-136	1
115-136*_H134[Z=5]	474.648	+5	2368.204	R_VIISA ¹²⁰ PSADAPMFVM ¹³⁰ GVNHEK	115-136	1
115-142**_H134[Z=2]	1545.281	+2	3088.547	R_VIISA ¹²⁰ PSADAPMFVM ¹³⁰ GVNHEK_YDNS ¹⁴⁰ LK	115-142	2
115-142**_H134[Z=3]	1030.523	+3	3088.547	R_VIISA ¹²⁰ PSADAPMFVM ¹³⁰ GVNHEK_YDNS ¹⁴⁰ LK	115-142	2
115-142**_H134[Z=4]	773.144	+4	3088.547	R_VIISA ¹²⁰ PSADAPMFVM ¹³⁰ GVNHEK_YDNS ¹⁴⁰ LK	115-142	2
115-142**_H134[Z=5]	618.717	+5	3088.549	R_VIISA ¹²⁰ PSADAPMFVM ¹³⁰ GVNHEK_YDNS ¹⁴⁰ LK	115-142	2
115-142**_H134[Z=6]	515.765	+6	3088.546	R_VIISA ¹²⁰ PSADAPMFVM ¹³⁰ GVNHEK_YDNS ¹⁴⁰ LK	115-142	2
116-136_H134[Z=2]	1107.058	+2	2212.101	VIISA ¹²⁰ PSADAPMFVM ¹³⁰ GVNHEK	116-136	0
116-136_H134[Z=3]	738.375	+3	2212.103	VIISA ¹²⁰ PSADAPMFVM ¹³⁰ GVNHEK	116-136	0
116-136_H134[Z=4]	554.033	+4	2212.103	VIISA ¹²⁰ PSADAPMFVM ¹³⁰ GVNHEK	116-136	0
116-142*_H134[Z=2]	1467.23	+2	2932.445	VIISA ¹²⁰ PSADAPMFVM ¹³⁰ GVNHEK_YDNS ¹⁴⁰ LK	116-142	1
116-142*_H134[Z=3]	978.489	+3	2932.445	VIISA ¹²⁰ PSADAPMFVM ¹³⁰ GVNHEK_YDNS ¹⁴⁰ LK	116-142	1
116-142*_H134[Z=4]	734.119	+4	2932.447	VIISA ¹²⁰ PSADAPMFVM ¹³⁰ GVNHEK_YDNS ¹⁴⁰ LK	116-142	1
116-142*_H134[Z=5]	587.497	+5	2932.449	VIISA ¹²⁰ PSADAPMFVM ¹³⁰ GVNHEK_YDNS ¹⁴⁰ LK	116-142	1
137-142[Z=1]	739.361	+1	738.354	YDNS ¹⁴⁰ LK	137-142	0
137-142[Z=2]	370.184	+2	738.353	YDNS ¹⁴⁰ LK	137-142	0
143-159_C149C153[Z=1]	1705.86	+1	1704.853	IVSNASCT ¹⁵⁰ TNCLAPLAK	143-159	0
143-159_C149C153[Z=2]	853.434	+2	1704.853	IVSNASCT ¹⁵⁰ TNCLAPLAK	143-159	0
143-159_C149C153[Z=3]	569.292	+3	1704.854	IVSNASCT ¹⁵⁰ TNCLAPLAK	143-159	0
160-183_H162H164H176[Z=2]	1309.691	+2	2617.367	V ¹⁶⁰ IHDHFGIVEG ¹⁷⁰ LMTTVHAITA ¹⁸⁰ TQK	160-183	0
160-183_H162H164H176[Z=3]	873.463	+3	2617.367	V ¹⁶⁰ IHDHFGIVEG ¹⁷⁰ LMTTVHAITA ¹⁸⁰ TQK	160-183	0
160-183_H162H164H176[Z=4]	655.349	+4	2617.367	V ¹⁶⁰ IHDHFGIVEG ¹⁷⁰ LMTTVHAITA ¹⁸⁰ TQK	160-183	0
160-183_H162H164H176[Z=5]	524.481	+5	2617.369	V ¹⁶⁰ IHDHFGIVEG ¹⁷⁰ LMTTVHAITA ¹⁸⁰ TQK	160-183	0
160-183_H162H164H176[Z=6]	437.235	+6	2617.366	V ¹⁶⁰ IHDHFGIVEG ¹⁷⁰ LMTTVHAITA ¹⁸⁰ TQK	160-183	0
184-191[Z=1]	760.383	+1	759.376	TVDGPSG ¹⁸⁰ K	184-191	0
184-191[Z=2]	380.695	+2	759.375	TVDGPSG ¹⁸⁰ K	184-191	0
192-194[Z=1]	474.282	+1	473.275	LWR	192-194	0
192-194[Z=2]	237.645	+2	473.275	LWR	192-194	0
195-212*[Z=2]	849.45	+2	1696.885	DGR_GAA ²⁰⁰ QNIIPASTGA ²¹⁰ AK	195-212	1
195-212*[Z=3]	566.636	+3	1696.886	DGR_GAA ²⁰⁰ QNIIPASTGA ²¹⁰ AK	195-212	1
198-212[Z=1]	1369.743	+1	1368.736	GAA ²⁰⁰ QNIIPASTGA ²¹⁰ AK	198-212	0
198-212[Z=2]	685.375	+2	1368.735	GAA ²⁰⁰ QNIIPASTGA ²¹⁰ AK	198-212	0
198-212[Z=3]	457.253	+3	1368.737	GAA ²⁰⁰ QNIIPASTGA ²¹⁰ AK	198-212	0
213-216[Z=1]	374.239	+1	373.232	AVGK	213-216	0
213-216[Z=2]	187.623	+2	373.231	AVGK	213-216	0
213-224*[Z=2]	612.869	+2	1223.723	AVGK_VIPE ²²⁰ LNGK	213-224	1
213-224*[Z=3]	408.915	+3	1223.723	AVGK_VIPE ²²⁰ LNGK	213-224	1
217-224[Z=1]	869.508	+1	868.501	VIPE ²²⁰ LNGK	217-224	0
217-224[Z=2]	435.258	+2	868.501	VIPE ²²⁰ LNGK	217-224	0
217-231*[Z=3]	549.308	+3	1644.902	VIPE ²²⁰ LNGK_LTGMAF ²³⁰ R	217-231	1
225-231[Z=1]	795.417	+1	794.410	LTGMAF ²³⁰ R	225-231	0
225-231[Z=2]	398.212	+2	794.409	LTGMAF ²³⁰ R	225-231	0

GAPDH Trypsin Digestion, continued

Name	Expected m/z	MS Charge (Z)	Monoisotopic Mass	Peptide Sequence	Sequence Position	Missed Cleavage
232-245_C244[Z=1]	1499.788	+1	1498.781	VPTPNVSVV ²⁴⁰ DLTCR	232 - 245	0
232-245_C244[Z=2]	750.398	+2	1498.781	VPTPNVSVV ²⁴⁰ DLTCR	232 - 245	0
232-245_C244[Z=3]	500.601	+3	1498.781	VPTPNVSVV ²⁴⁰ DLTCR	232 - 245	0
232-248*_C244[Z=2]	935.508	+2	1869.001	VPTPNVSVV ²⁴⁰ DLTCR_LEK	232 - 248	1
232-248*_C244[Z=3]	624.008	+3	1869.002	VPTPNVSVV ²⁴⁰ DLTCR_LEK	232 - 248	1
246-248[Z=1]	389.239	+1	388.232	LEK	246 - 248	0
246-248[Z=2]	195.123	+2	388.231	LEK	246 - 248	0
246-251*[Z=1]	659.408	+1	658.401	LEK_AA ²⁵⁰ K	246 - 251	1
246-251*[Z=2]	330.208	+2	658.401	LEK_AA ²⁵⁰ K	246 - 251	1
249-256*[Z=2]	462.245	+2	922.475	AA ²⁵⁰ K_YDDIK	249 - 256	1
249-257**[Z=2]	526.292	+2	1050.569	AA ²⁵⁰ K_YDDIK_K	249 - 257	2
249-257**[Z=3]	351.197	+3	1050.569	AA ²⁵⁰ K_YDDIK_K	249 - 257	2
252-256[Z=1]	653.313	+1	652.306	YDDIK	252 - 256	0
252-256[Z=2]	327.16	+2	652.305	YDDIK	252 - 256	0
252-257*[Z=1]	781.408	+1	780.401	YDDIK_K	252 - 257	1
252-257*[Z=2]	391.208	+2	780.401	YDDIK_K	252 - 257	1
258-260[Z=1]	345.249	+1	344.242	VVK ²⁶⁰	258 - 260	0
261-268[Z=1]	829.441	+1	828.434	QASEGPLK	261 - 268	0
261-268[Z=2]	415.224	+2	828.433	QASEGPLK	261 - 268	0
307-320[Z=1]	1763.802	+1	1762.795	LISW ³¹⁰ YDNEFGYSNR ³²⁰	307 - 320	0
307-320[Z=2]	882.405	+2	1762.795	LISW ³¹⁰ YDNEFGYSNR ³²⁰	307 - 320	0
307-320[Z=3]	588.606	+3	1762.796	LISW ³¹⁰ YDNEFGYSNR ³²⁰	307 - 320	0
321-331_H327[Z=1]	1229.637	+1	1228.630	VVDLMVHMAS ³³⁰ K	321 - 331	0
321-331_H327[Z=2]	615.322	+2	1228.629	VVDLMVHMAS ³³⁰ K	321 - 331	0
321-331_H327[Z=3]	410.551	+3	1228.631	VVDLMVHMAS ³³⁰ K	321 - 331	0
321-332*_H327[Z=1]	1358.68	+1	1357.673	VVDLMVHMAS ³³⁰ K_E	321 - 332	1
321-332*_H327[Z=2]	679.844	+2	1357.673	VVDLMVHMAS ³³⁰ K_E	321 - 332	1
321-332*_H327[Z=3]	453.565	+3	1357.673	VVDLMVHMAS ³³⁰ K_E	321 - 332	1

Gradients for peptide separation

The following gradients were applied to separate tryptic peptides:

Gradient A: MB-sensitized photolysis

flow rate = 5 μ l
injection volume = 3 μ l

Mobile phases

time	Mobile phases	
	A: MQ + 10%ACN + 0.1%FA	B: ACN + 0.1%FA
0	100%	
3	100%	
40	75%	25%
45	55%	45%
50	30%	70%
58	30%	70%
60	100%	
70	100%	

Gradient B: All other photolyses

flow rate = 5 μ l
injection volume = 3 μ l

Mobile phases

time	Mobile phases	
	A: MQ + 3%ACN + 0.1%FA	B: ACN + 0.1%FA
0	100%	
6	100%	
55	70%	30%
65	30%	70%
75	30%	70%
77	100%	
87	100%	